学位論文

Observing the Weak Value through Quantum Interference
(量子干渉を通して観る弱値)

平成26年12月博士（理学）申請

東京大学大学院理学系研究科
物理学専攻
森 琢也

Abstract

In quantum mechanics, it is well known that counterfactual arguments sometimes lead to paradoxes, which implies that our classical intuition is not always reliable. However, it has been pointed out by several authors that the weak value, which was introduced by Aharonov et al. in 1988, may be useful to comprehend quantum mechanics intuitively. Another extraordinary aspect of the weak value is its amplification, which has been exploited for precision measurement. Nevertheless, the physical meaning of the weak value is still obscure due to its complexity of the value and the very fact of the amplification. In this thesis, by considering various situations of quantum interference, we attempt to provide a possible interpretation of the weak value. We find, on one hand, that the imaginary part of the weak value is relevant to the wave nature. On the other hand, in the double-slit experiment the particle nature can be seen in the real part of the position weak value. This property for the real part does not hold for more general cases such as the multiple (more than two) slit experiment. The position weak value, nevertheless, can be interpreted as the average of the classical trajectories based on a complex probability. We also investigate the possibility of knowing which path the particle takes in the multiple-slit experiment without destroying the interference fringes. We show that, because of the statistical nature of the weak value, obtaining the which-path information and the interference pattern is compatible with complementarity. Our study suggests that the weak value is a reasonable physical quantity.

Contents

Chapter 1

Introduction

In quantum mechanics, defining the trajectory of a particle is considered to be impossible due to the uncertainty principle. In fact, one of the most intriguing features of quantum mechanics is the wave-particle duality which can be observed in the double-slit experiment, and we all know that the measurement of the which-path information destroys the interference pattern on the screen (i.e., the complementarity).

In 1924, de Broglie introduced the matter wave (de Broglie wave) as an attempt to achieve a physical synthesis of the wave nature and the particle nature [1]. At the 5th Solvay conference, Einstein's main concern was whether the causality of the space-time holds in quantum mechanics, which resulted in the impressive discussion on the famous two-slit thought experiment. If one performs the double-slit experiment by using many electrons, an interference pattern appears on the screen. Intermediately, the particle should go through one of the slit, and one can measure the transversal momentum of the slit when the particle passes the slit. Naturally, the total momentum must be conserved, and the momentum that the particle loses (or gets) can be deduced. It follows that, from the position of the particle at the screen, which path the particle took can also be found. Einstein pointed out that obtaining both which-path information and the interference pattern contradicts the complementarity. In response, Bohr stated that the measurement system, too, must obey quantum mechanics and, if one performs the which path experiment, it will destroy the interference due to the uncertainty relation, and vice versa. Bohr asserted that, in quantum mechanics, specifying the measurement apparatus is essential, and we should not employ two contradicting measurements. Later, Feynman mentioned that

> *this is impossible, absolutely impossible, to explain in any classical way, and which has in it the heart of quantum mechanics* [2].

The double-slit experiment with the electron was demonstrated in 1965 by Jönsson [3], and the supplementary examination has been performed by Tonomura in 1989 [4], who is also known for the experiment of the Aharonov-Bohm effect [5, 6]. While the apparatus suggested by Einstein at the 5th Solvay conference is designed to find which path the particle takes by measuring the momentum of the slit, Scully et al. proposed an ingenious experiment which allows us to determine the which-path information without transferring the momentum of the

particle, and also suggested how to erase the which-path information [7]. Their conclusion, however, is the same as that obtained by the Bohr-Einstein debate, that is, no one can observe its trajectory and interference simultaneously.

Despite this, the reconstruction of the trajectories in the double-slit experiment has been demonstrated by Kocsis et al. [8] by the approach based on the weak value argued by Wiseman [9]. In the de Broglie-Bohm theory, the velocity of the particle (the derivative of the position with respect to time) is defined, and Wiseman pointed out that this velocity is naturally related to the real part of the momentum weak value. Intermediately, they measured the weak value of the momentum for a number of different screen positions and performed many trials to reconstruct the trajectory. The resultant trajectories agree with the prediction of the de Broglie-Bohm theory [10, 11, 12]. As Kocsis et al. claimed, the trajectories are reconstructed by using a large number of photons, i.e., the trajectories are defined by an ensemble, not by an individual event. The de Broglie-Bohm theory is one of the most successful examples of hidden variable theory, which is meant to describe all physical processes through the particle nature. In the de Broglie-Bohm theory, the motion of a particle must obey what is called "quantum potential" and, if one knows the particle's initial position, its motion is completely determined [10, 11]. If, however, one measures the initial position of the particle, the position of the particle is completely disturbed. Thus, the de Broglie Bohm theory allows us to infer its initial position by measuring its final position.

The weak value, which was proposed by Aharonov et al. in 1988 [13], is a value defined by two boundary conditions. Weak values are defined in the framework of quantum mechanics and can be seen as a generalization of the expectation value, in the sense that the weak value coincides with the expectation value if we choose the two boundaries by the same state. Like the expectation value, the weak value is also a statistical value. The definition of the weak value is similar to that of the S-matrix because the initial state evolves under the Hamiltonian until the final state is specified. The main difference between the S-matrix and the weak value is that the interaction does not disturb the initial state in the weak limit. We call these initial- and final states pre- and post-selected states, respectively. The measurement is performed in such a way that the object system is minimally disturbed.

Since the weak value can exceed the range of the eigenvalues, one has the possibility of amplification and may be applied to precise measurement, i.e., estimating a tiny coupling constant which cannot be measured in the conventional method [14, 15]. Also, the wave function can be experimentally measured by using the weak value [16]. Besides these applications, weak values can be applied to explain away several quantum paradoxes.

Our conclusion deduced from some counterfactual argument (reference to the measurement that we actually do not perform) sometimes fails to explain the actual result, and Hardy proposed the Mach-Zehnder type interferometers to explain his paradox [17]. In Hardy's paradox, two Mach-Zehnder interferometers are implemented, and instead of a photon, an electron and a positron are used for each interferometer. The interferometers have an overlapping part, and if the electron and the positron enter the overlapping path simultaneously, they must be annihilated. The electron always arrives at one of the detectors without the positron, and vice versa. However, due to the overlap, the other detector can also click. One may infer that, when the other detectors click simultaneously, the electron and the positron are

taking the overlapping path. Apparently, this result contradicts the assumption that, if both the electron and the positron take the overlapping path, they must annihilate each other on the overlapping path. As Bohr pointed out that the physical value is dependent on the measurement setup. Without measurement, we must not infer its intermediate state. Since counterfactual statements are not allowed in quantum mechanics, intuitive explanations are not always eligible to deduce correct conclusions. The weak measurement, however, is expected to provide reasonable explanations for quantum mechanics. Indeed, for examples, to explain Hardy's paradox, the weak measurement has been applied [18, 19, 20].

As another example, recently Danan et al. proposed that the weak value gives a reasonable explanation for experimental outcomes obtained in a nested Mach-Zehnder interferometers [21]. In order to infer the path that the photons take, each mirror vibrates around its horizontal axes with a certain frequency. Inference by the evolving state from the initial state does not coincide with the measurement result (counterfactual measurement), but Danan et al. suggested that inference by backwardly evolving state from the final state may be necessary to understand this measurement result intuitively, and their conclusion is consistent with the two-state vector formulation of quantum mechanics [22, 23]. By using weak values, another intriguing example has been proposed and demonstrated in a recent experiment, in which the spin-1/2 nature is separated from the particle [24, 25].

The physical meaning of the weak value, however, is still obscure because of the complexity of its value and its possible amplification. Among several papers attempting to figure out the physical interpretation for the weak value, Aharonov and Botero express the weak value as

> *the weak value can be regarded as a definite mechanical effect on a measuring probe specifically designed to minimize the back reaction on the measured system* [26].

Similarly, Dressel and Jordan interpret the weak value as

> *the real part of the weak value stems directly from the part of the conditioned shift of the detector pointer. The imaginary part stems directly from the disturbance of the measurement* [27].

The interpretation of the real and imaginary parts of the weak values proposed by Dressel and Jordan is based on the canonical commutation relation. They concluded that the imaginary part of the weak value is derived from the post-selection, and the real part can be seen as the conditional average. Aharonov and Dressel claimed that the weak value can be interpreted in terms of the mechanical effect of the measurement. Vaidman, one of the proponents of the weak value, stated that there is a significant meaning in the weak value:

> *our definition of elements of reality, i.e., a definite shift of the probability distribution of the pointer variable yields for pre-and post-selected systems the weak value* [28].

Vaidman, in his paper, proposed a novel definition of an element of reality and asserted that, when the interaction between the object and a meter system is weak, the average shift of the

meter (which is the weak value if one performs the post-selection) coincides with the element of reality. The standpoint of Vaidman is different from that of Aharonov and Dressel, because the mechanical shift of the meter has been given a distinguished meaning, namely, the element of reality.

In our paper, we adopt a similar position as Vaidman without relying on the notion of an element of reality. Instead, we try to find a proper interpretation of the weak value through several examples. We utilize the weak value so as to understand quantum mechanics intuitively. The difficulty of defining a trajectory in quantum mechanics is known: when the position of the particle is determined, the momentum becomes completely unknown, making the trajectory completely ambiguous. Since the weak value is obtained in the weak limit, ideally speaking, the initial (pre-selected) state is not disturbed, even if the position is observed. Besides, the position weak value coincides with the classical trajectory in several examples, so that utilizing the position weak value as the (weak) trajectory is reasonable. In the double-slit experiment, the position weak value can be obtained without destroying the interference pattern. In our paper, we investigate the interference effect based on the weak values.

We show that the interference effect can be expressed in terms of the imaginary part of the weak value [29]. In contrast, in the double-slit experiment, the real part of the position weak value can be interpreted as a particle picture. However, this particle nature does not hold for the multiple-slit experiment. Nevertheless, we can show that the position weak value can be realized as the average of the classical trajectory based on the complex probability. By introducing the internal degree of freedom, the classical trajectory is obtained from the re-scaled weak value without destroying the interference pattern. This trajectory does not contradict the complementarity because the weak value is statistical [29, 30].

The plan of this paper is as follows. In chapter 2, we quickly review several examples to learn how to utilize the weak value in terms of the intuitive interpretation, and how to perform the weak measurement. Then, the connection between interference and the imaginary part of the weak value is shown in chapter 3. The index of interference is defined and expressed in terms of the imaginary part of the weak value. This way, the imaginary part of the weak value can be related to the interference effect [29]. As examples, we treat the double-slit (thought) experiment and the spin-1/2 system. It turns out that the index of interference can be expressed in terms of the imaginary part of the momentum weak value. The index of interference can be expressed in terms of the imaginary part of the spin component. In chapter 4 we investigate the trajectory in terms of the position weak value by using multiple-slit (thought) experiment and Lloyd's mirror experiment. In the free Hamiltonian, the position weak value of the particle between two points exactly coincides with the classical trajectory. This feature, however, does not hold in the double-slit experiment because there exists an imaginary part. The real part is the average of the classical trajectories. However, again, this property does not hold when we consider the three- (or multiple-) slit experiment. Admitting the complex probability, the position weak value can be interpreted as the average of the classical trajectory. In classical optics, Lloyd's mirror experiment is known for making the interference pattern on the screen with a single slit. The position weak value can be calculated, and the result shows that the weak trajectory is a smooth function of time t and has the

imaginary part which cannot be seen in classical optics. Also, the spin-tagged position weak value is defined in order to specify which path the particle takes without destructing the interference by exploiting quantum eraser. The re-scaled spin-tagged weak value coincides with the classical trajectory. We show that this spin-tagged position weak value does not contradict the complementarity [29, 30]. Our conclusion and discussions are provided in chapter 5. Detailed calculation in section 2.5 is in Appendix A. In Appendix B, we show that, for the double-slit experiment for quantum eraser, the index of interference is represented by the imaginary part of the spin-tagged momentum weak value.

This thesis is based on the submitted papers [29, 30].

Chapter 2

Weak value and the weak measurement

In this chapter, we briefly review the weak value and its applications. The weak value was proposed by Aharonov et al. in 1988 [13]. The weak value can be implemented in precision measurement [14, 15] and be used to explain quantum paradoxes [19, 21]. The trajectories of particles are reconstructed from the momentum weak value [8, 9], and reconstructed trajectories coincide with the prediction of the de Broglie-Bohm theory [10, 11, 12]. Nonetheless, because of the amplification and the complex valuedness of the weak value, the physical meaning of the weak value is still obscure. Several authors attempted to find a physical interpretation for the weak value [26, 27, 28]. The weak measurement is utilized to obtain the weak value.

2.1 Time symmetry in the quantum process of measurement

Before taking up the argument of the weak value, we briefly explain time symmetry in the quantum process of measurement (two-state vector formalism) [22]. This procedure was advocated by Aharonov et al. and closely connected to the weak value. Reznik and Aharonov claimed that the weak value is a physical quantity in the time-symmetric process [31].

In quantum mechanics, the dynamical laws of motion, which can be expressed by either the Heisenberg equation or the Schrödinger equation, are time symmetric and correspond to Hamilton's equation of motion in classical mechanics. However, the macroscopic phenomena are, of course, asymmetric in time, e.g., the second law of thermodynamics. It is believed that asymmetric phenomena enter into quantum mechanics through the theory of measurement which cannot be described by the Heisenberg equation nor the Schrödinger equation. The measurement induces the wave function collapse which is time irreversible. Aharonov et al. introduced time symmetric nature into the measurement theory [22]. The initial state is selected by a measurement (pre-selection). In conventional theory, one performs the measure-

ment on this initial state. In the two-state vector formalism, however, the selection of the final state (post-selection) is also required, and the future and the past should be considered equivalently. The initial state is prepared by the measurement A_0 (pre-selection), and when the measurement result is a_0^i, the corresponding state is assumed to be $|a_0\rangle$. The superscript "i" denotes distinct eigenvalues of the observable, and the subscript denotes different observable. The final state is selected by the measurement A_{N+1} (post-selection), and when the outcome is a_{N+1}^n, the corresponding state is $|a_{N+1}\rangle$. Intermediately the N measurements, $A_1, A_2, \ldots, A_N$, are implemented. The results, $a_1^j, a_2^k, \ldots, a_N^m$, are obtained, and the corresponding eigenstates are described by $|a_1^j\rangle, |a_2^k\rangle, \ldots, |a_N^m\rangle$, respectively. The projection operator is expressed by,

$$\Pi_j^i = |a_j^i\rangle\langle a_j^i|. \tag{2.1}$$

The joint probability $P(a_0^i, a_1^j, \ldots, a_{N+1}^n)$ that the measurements $A_0, A_1, \cdots, A_N, A_{N+1}$ result in the eigenvalues $a_0^i, a_1^j, a_2^k, \ldots, a_N^m, a_{N+1}^n$ is defined by

$$P(a_0^i, a_1^j, \ldots, a_{N+1}^n) := \mathrm{Tr}(\Pi_0^i \Pi_1^j \Pi_2^k \cdots \Pi_N^m \Pi_{N+1}^n \Pi_N^m \Pi_{N-1}^l \cdots \Pi_1^j). \tag{2.2}$$

The total probability $P(a_0^i, a_{N+1}^n)$ is defined by taking all possible summation for the intermediate states:

$$P(a_0^i, a_{N+1}^n) := \sum_i \sum_j \cdots \sum_n \mathrm{Tr}(\Pi_0^i \Pi_1^j \Pi_2^k \cdots \Pi_N^m \Pi_{N+1}^n \Pi_N^m \Pi_{N-1}^l \cdots \Pi_1^j). \tag{2.3}$$

The conditional probability $P(a_1^j, \ldots, a_N^m | a_0^i, a_{N+1}^n)$ that the outcomes $a_1^j, \ldots, a_N^m$ are obtained for fixed values a_0^i and a_N^n is given by

$$P(a_1^j, \ldots, a_N^m | a_0^i, a_{N+1}^n) = \frac{P(a_0^i, a_1^j, \ldots, a_{N+1}^n)}{P(a_0^i, a_{N+1}^n)}. \tag{2.4}$$

The conditional probability $P(a_1^j, \ldots, a_N^m | a_0^i, a_{N+1}^n)$ is time symmetric because, if one performs the measurement backward in time, i.e., $A_{N+1}, A_N, \cdots, A_1$, the conditional probability does not change. Some may wonder that the post-selection is artificial. However, this kind of procedure is implemented by the experimenter. For example, let us consider the Stern-Gerlach experiment. Firstly, the ensemble of particles with the spin z up is prepared by the measurement (pre-selection). Then, the measurement of the spin component along x (or y) is measured (intermediate measurement). Finally, the experimenter should count the number of particle at the screen (post-selection). Thus, the experimenter performs the pre- and post-selections.

2.2 Weak value

The definition of the weak value of the observable A is

$$A_w = \frac{\langle\psi|A|\phi\rangle}{\langle\psi|\phi\rangle}, \tag{2.5}$$

where $|\phi\rangle$ and $|\psi\rangle$ are the pre- and post-selected states, respectively [13]. The weak value A_w can be seen as a generalized expectation value because, if one puts the post-selected state as $|\psi\rangle = |\phi\rangle$, the expectation value can be obtained from the weak value. The expectation value can also be obtained from the weak value by using the completeness relation $\sum_\psi |\psi\rangle\langle\psi| = \mathbb{I}$,

$$\begin{aligned}\langle A\rangle &:= \langle\phi|A|\phi\rangle = \sum_\psi \langle\phi|\psi\rangle\langle\psi|A|\phi\rangle = \sum_\psi |\langle\psi|\phi\rangle|^2 \frac{\langle\psi|A|\phi\rangle}{\langle\psi|\phi\rangle} \\ &= \sum_\psi |\langle\psi|\phi\rangle|^2 A_w, \end{aligned} \tag{2.6}$$

where $|\langle\psi|\phi\rangle|^2$ is the probability to obtain the post-selected state $|\psi\rangle$ for a given pre-selected state $|\phi\rangle$. It is clear that, when the denominator of (2.5), $\langle\psi|\phi\rangle$, approaches to zero, the weak value becomes infinitely large unless the numerator also becomes zero (amplification). Besides, the weak value is a complex valued number because of the post-selection. Due to the amplification and the complex valuedness of the weak value, the physical meaning of the weak value is obscure.

The amplification of the weak value may be applied to estimate the coupling constant which cannot be detected in the conventional method [14, 15]. The weak value also allows us to measure the wave function directly [16]. Besides, it is expected that the weak value enables us to explain the measurement result intuitively [18, 19, 20]. In quantum mechanics, as Bohr described, we cannot mention the counterfactual measurement that we do not measure, and the conclusion based on the counterfactual measurement sometimes leads to the paradox as Hardy's paradox [17]. By exploiting the weak value, however, the reasonable explanation can be obtained. A bizarre feature of the weak value can also be observed, in which the spin-1/2 nature is separated from the particle by using neutrons [24, 25].

We summarize the applications of the weak values in the following sections.

2.2.1 Hardy's paradox

In this subsection, we briefly explain Hardy's paradox, and the intuitive interpretation of Hardy's paradox is shown by exploiting the weak value. Hardy's paradox directly stems from the counterfactual measurement [17]. As Bohr noted, in quantum mechanics, all we can mention is the measurement result. Meanwhile, Aharonov et al. claimed that the weak value can be applied to explain away Hardy's paradox [19].

Hardy utilized two Mach-Zehnder interferometers to explain his paradox [17]. Each interferometer has the overlapping part, and instead of photons, electrons (e^-) and positrons (e^+) are exploited. Without a particle e^+ (e^-), another particle e^- (e^+) always arrives at the detector C_- (C_+) (see Fig. 2.1). When each particle gets through the overlapping path, the particles must be annihilated. The electron state passing through on the overlapping path is described by $|o\rangle_-$ and the positron state on the overlapping path, is described by $|o\rangle_+$. In contrast, if the electron and the positron are on the non-overlapping paths, these states are

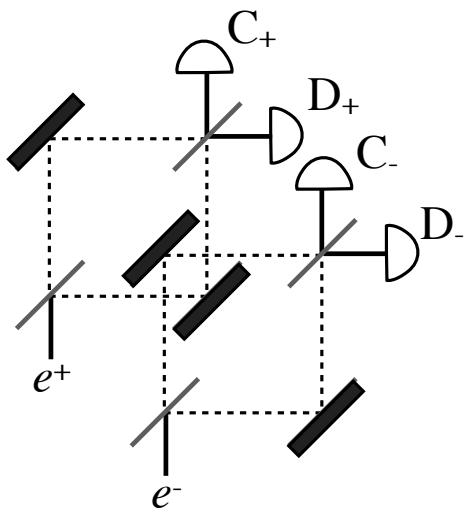

Figure 2.1: The illustration for Hardy's paradox in which the combination of two Mach-Zehnder interferometers is employed. Each interferometer is set to arrive at the $C_{\pm}$. When both particles get through the overlapping path simultaneously, the particles annihilated, so that the probability that the detector $D_{\pm}$ clicks is not zero.

represented by $|no\rangle_-$ and $|no\rangle_+$, respectively. The initial state is denoted by

$$|\phi\rangle = \frac{1}{\sqrt{3}}(|o\rangle_+ \otimes |no\rangle_- + |no\rangle_+ \otimes |o\rangle_- + |no\rangle_+ \otimes |no\rangle_-), \tag{2.7}$$

when the particles are not annihilated. It is assumed that the detector $D_+(D_-)$ clicks whenever the electron or the electron (the positron) enters the overlapping path. If $|\phi\rangle$ is projected onto the positron state $|no\rangle_+$ (the positron goes through the non-overlapping path), the electron state is ${}_+\langle no|\phi\rangle \propto (|o\rangle_- + |no\rangle_-)/\sqrt{2}$, and then the detector C_- clicks. Similarly, the detector C_+ clicks when the positron state is ${}_-\langle no|\phi\rangle \propto (|o\rangle_+ + |no\rangle_-)/\sqrt{2}$ (the electron goes through the non-overlapping path). The detectors D_- and D_+ click when the electron and the positron states are $(|o\rangle_- - |no\rangle_-)/\sqrt{2}$ and $(|o\rangle_+ - |no\rangle_+)/\sqrt{2}$, respectively. The joint probability that the detector C_+ and C_- click simultaneously is

$$P(C_+, C_-) = \frac{3}{4}. \tag{2.8}$$

In the same vein, the joint probabilities $P(C_+, D_-), P(D_+, C_-), P(D_+, D_-)$ are

$$P(C_+, D_-) = P(D_+, C_-) = P(D_+, D_-) = \frac{1}{12}. \tag{2.9}$$

The joint probability $P(D_+, D_-)$ that the detectors $D_{\pm}$ click simultaneously is not zero. When D_+ and D_- click simultaneously, both of the particle take the overlapping path (because it is

assumed that the detector $D_\pm$ clicks when either the electron or the positron enters overlapping path), and it contradicts the fact that the electron and the positron must be annihilated.

Next, let us show that the weak value can be exploited to explain Hardy's paradox intuitively [19]. Our interest is when D_+ and D_- click simultaneously, and hence we choose the post-selected state as

$$|\psi\rangle = \frac{1}{2}(|no\rangle_+ - |o\rangle_+) \otimes (|no\rangle_- - |o\rangle_-). \tag{2.10}$$

We define the projection operators,

$$\Pi^+_{no} = |no\rangle_{++}\langle no|, \quad \Pi^-_{no} = |no\rangle_{--}\langle no|, \tag{2.11}$$
$$\Pi^+_{o} = |o\rangle_{++}\langle o|, \quad \Pi^-_{o} = |o\rangle_{--}\langle o|, \tag{2.12}$$
$$\Pi^{+,-}_{no,o} = \Pi^+_{no} \otimes \Pi^-_{o}, \quad \Pi^{+,-}_{o,o} = \Pi^+_{o} \otimes \Pi^-_{o}, \tag{2.13}$$
$$\Pi^{+,-}_{o,no} = \Pi^+_{o} \otimes \Pi^-_{no}, \quad \Pi^{+,-}_{no,no} = \Pi^+_{no} \otimes \Pi^-_{no}, \tag{2.14}$$

from which the path of the particles can be obtained, e.g., the operator Π^+_{no} expresses that the positron is on the non-overlapping path. The weak value of the projection operators (2.11), (2.12) can be easily derived as

$$\Pi^-_{o_w} = \frac{\langle\psi|\Pi^-_{o_w}|\phi\rangle}{\langle\psi|\phi\rangle} = 1, \quad \Pi^+_{o_w} = \frac{\langle\psi|\Pi^+_{o_w}|\phi\rangle}{\langle\psi|\phi\rangle} = 1, \tag{2.15}$$
$$\Pi^-_{no_w} = \frac{\langle\psi|\Pi^-_{no_w}|\phi\rangle}{\langle\psi|\phi\rangle} = 0, \quad \Pi^+_{no_w} = \frac{\langle\psi|\Pi^+_{no_w}|\phi\rangle}{\langle\psi|\phi\rangle} = 0, \tag{2.16}$$

from which we can conclude neither the positron nor the electron takes non-overlapping path in terms of the weak value. It is consistent with the intuitive argument. Similarly, the weak values of the projection operators (2.13), (2.14) are obtained,

$$\Pi^{+,-}_{o,o_w} = 0, \tag{2.17}$$
$$\Pi^{+,-}_{no,o_w} = 1, \ \Pi^{+,-}_{o,no_w} = 1, \tag{2.18}$$
$$\Pi^{+,-}_{no,no_w} = -1, \tag{2.19}$$

from which we conclude that the electron and the positron do not take the overlapping path simultaneously. Besides, from (2.18), we conclude that the electron (the positron) gets through the overlapping path while the positron (the electron) gets through the non-overlapping path. However, it is weird because there is always only one pair. To compensate this discrepancy, (2.19) can be implemented. Both particles take non-overlapping paths.

Hardy's paradox is originated from the inference of the counterfactual measurement. Even if the detectors D_+ and D_- click simultaneously, one cannot conclude that the particles get through the overlapping path. However, the weak value may enable us to mention the intermediate state and give us the intuitive explanation.

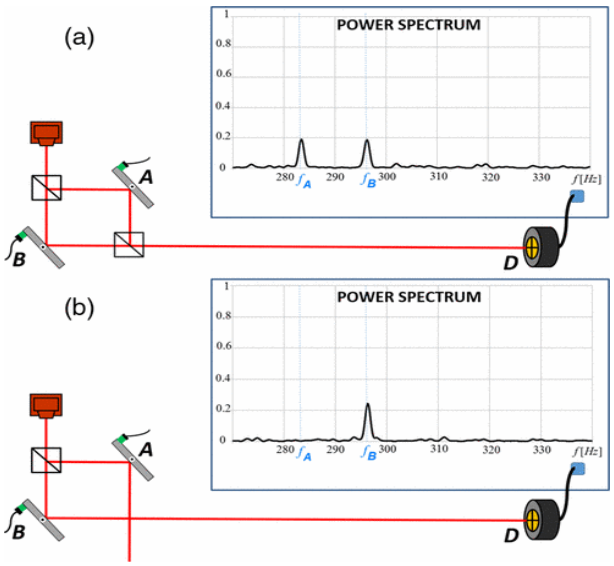

Figure 2.2: FIG. 1 from [21]. Mirrors A and B are rotating horizontally with frequencies f_A and f_B, respectively. Red lines represent the path that the photons take. (a): Mach-Zehnder interferometer with the power spectrum. (b): Mach-Zehnder interferometer without the second beam splitter. Only the frequency f_B is measured.

2.2.2 Asking photons where they have been

Danan et al. suggested the intuitive interpretation of the Mach-Zehnder interferometer by using weak values [21].

Firstly, a simple Mach-Zehnder interferometer is considered. Mirrors A and B vibrate horizontally with frequencies f_A and f_B, respectively. Intuitively, from Fig. 2.2 (a) photons are passing through both arms, and the measurement result coincides with this intuition. When the second beam splitter of the interferometer is removed, intuitively, the detected photons pass through one of the arms, and the intuitive inference is consistent with the measurement result: Fig. 2.2 (b).

Secondly, more complicated interferometer is suggested as Fig. 2.3 (a), (b), and (c). In Fig. 2.3 (a), the interferometer is prepared so that the photons may be passing through all arms, and the power spectrum explains that the photons are affected by all mirrors. So far, it seems that the intuitive explanation (the path of the photons) coincides with the measurement result. In general, however, this intuitive explanation does not work. The interferometer is adjusted so that the photons are not to reach the mirror F as Fig. 2.3 (b). Intuitively, the only detected photons are passing through the mirror C while the photons that take the path via the mirrors E, A, and B, do not reach the detector, and hence it seems that the only frequency f_C would be detected. However, from the measurement result Fig. 2.3 (b), the frequencies f_A, f_B, and f_C are detected. Besides, the frequency f_E is not detected even though the frequencies f_A and f_B are measured. This result (the power spectrum) contradicts the intuition. This discrepancy occurs due to the counterfactual intuition. One may think

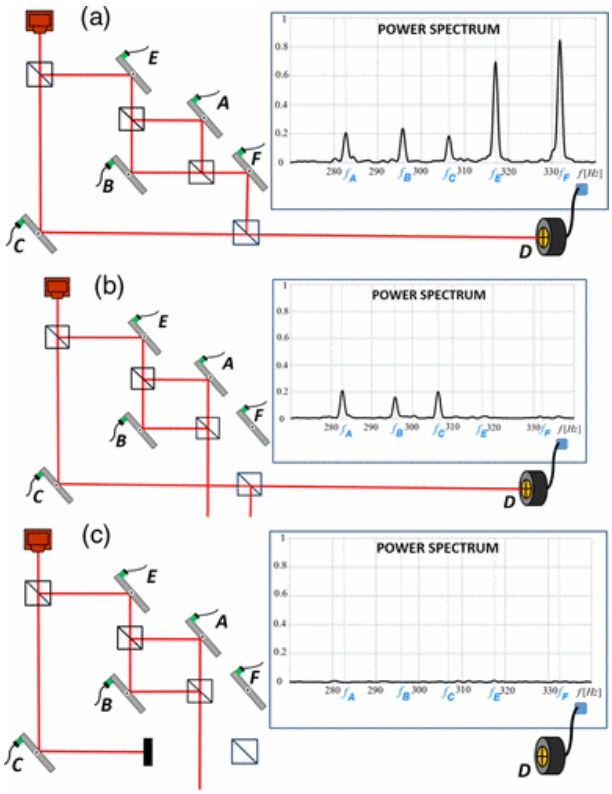

Figure 2.3: FIG. 2 from [21]. Each mirror are oscillating horizontally with certain frequencies. Red lines represent the path that the photons take. (a): Mach-Zehnder interferometer with the power spectrum. All frequencies are detected. (b): Set inner interferometer not to reach at the detector. (c): No frequencies are detected when the lower arm is blocked.

that some of the particles leak to the mirror F and are detected. To check this, Danan et al. performed the measurement as shown in Fig. 2.4 (c), and it turns out that there are no leak.

Danan et al. suggested that the result in Fig. 2.3 (b) can be explained in terms of the weak values. The localized wave packet near the mirror A is described by $|A\rangle$, etc. The pre-selected state is

$$|\phi\rangle = \frac{1}{\sqrt{3}}(|A\rangle + \mathrm{i}|B\rangle + |C\rangle). \tag{2.20}$$

The post-selected state is

$$|\psi\rangle = \frac{1}{\sqrt{3}}(|A\rangle - \mathrm{i}|B\rangle + |C\rangle). \tag{2.21}$$

Let us define several projection operators,

$$\Pi_A = |A\rangle\langle A|,\ \Pi_B = |B\rangle\langle B|, \tag{2.22}$$
$$\Pi_C = |C\rangle\langle C|,\ \Pi_E = |E\rangle\langle E|, \tag{2.23}$$
$$\Pi_F = |F\rangle\langle F|, \tag{2.24}$$

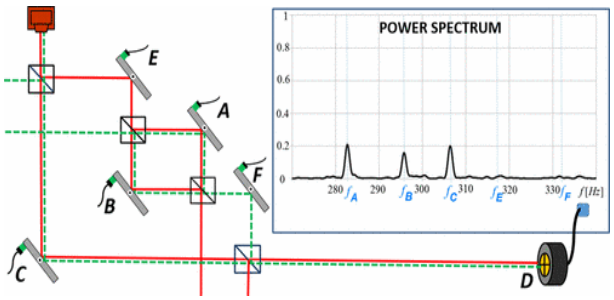

Figure 2.4: FIG. 3 from [21]. Describing two-state vector formalism. Each mirror oscillates horizontally with a different frequency. Red lines represent the path that the photons take. Dashed green lines represent the backward evolving state.

from which one can observe the path of the photons. The weak values are

$$\Pi_{A_w} = \frac{\langle\psi|A|\phi\rangle}{\langle\psi|\phi\rangle} = 1, \quad \Pi_{C_w} = \frac{\langle\psi|C|\phi\rangle}{\langle\psi|\phi\rangle} = 1, \tag{2.25}$$

$$\Pi_{B_w} = \frac{\langle\psi|B|\phi\rangle}{\langle\psi|\phi\rangle} = -1, \tag{2.26}$$

$$\Pi_{E_w} = \frac{\langle\psi|E|\phi\rangle}{\langle\psi|\phi\rangle} = 0, \quad \Pi_{F_w} = \frac{\langle\psi|F|\phi\rangle}{\langle\psi|\phi\rangle} = 0, \tag{2.27}$$

and these values correspond to the measurement result in Fig. 2.3 (b) except for its sign. Also, the result Fig. 2.3 (b) can be explained in terms of the two-state vector formalism of quantum theory [22]. Let us consider the post-selected state $|\psi\rangle$ which evolves backward in time. The path that photons take is indicated by dashed green lines in Fig. 2.4. We may conclude that the power spectrum can be intuitively explained away by the overlapping of the states evolving forward and backward. Danan et al. concluded that, in order to give reasonable explanation for the measurement, one has to take into account the backward evolving state, not only the forward evolving state.

2.2.3 Cheshire cat

Aharonov et al. proposed a "quantum Cheshire cat" [24] making an analogy to *Alice's Adventures in Wonderland* written by Lewis Carroll in which the Cheshire cat disappears while its grin is left. Aharonov et al. suggested that, in terms of the weak value, the grin is separated from the Cheshire cat. In this subsection, we briefly review the quantum Cheshire cat, which is realized by using the weak value [24].

The locations of the cat in the box 1 and the box 2 are represented by $|1\rangle$ and $|2\rangle$, respectively. The state that the cat is grinning is expressed by $|+\rangle$, while $|-\rangle$ represents the cat with frowning. Let us introduce projection operators for the grin state and the frown state as

$$\Pi_+ \equiv |+\rangle\langle+|, \quad \Pi_- \equiv |-\rangle\langle-|, \tag{2.28}$$

from which whether the cat is grinning or not can be observed. The cat with grin is expressed by

$$\sigma_z := \Pi_+ - \Pi_-. \tag{2.29}$$

For the location of the cat, the projection operator is described by

$$\Pi_1 \equiv |1\rangle\langle 1|,\ \Pi_2 \equiv |2\rangle\langle 2|, \tag{2.30}$$

from which the position of the cat can be observed. At $t = 0$, initially the cat state is prepared as,

$$|\phi\rangle = \frac{1}{2}(|+\rangle + |-\rangle) \otimes |1\rangle + \frac{1}{2}(|+\rangle - |-\rangle) \otimes |2\rangle, \tag{2.31}$$

and at $t = T$, the cat state is post-selected by

$$|\psi\rangle = \frac{1}{2}(|+\rangle - |-\rangle) \otimes (|1\rangle + |2\rangle). \tag{2.32}$$

The location of the cat and whether the cat is grinning are obtained in terms of the weak values,

$$\Pi_{1_w} = \frac{\langle\psi|\Pi_1|\phi\rangle}{\langle\psi|\phi\rangle} = 0, \tag{2.33}$$

$$\Pi_{2_w} = \frac{\langle\psi|\Pi_2|\phi\rangle}{\langle\psi|\phi\rangle} = 1, \tag{2.34}$$

$$\sigma_{z_w} = \frac{\langle\psi|\sigma_z|\phi\rangle}{\langle\psi|\phi\rangle} = 1, \tag{2.35}$$

from which the cat is always grinning and in the box 2 intermediately, and one may infer that the cat is in the box 2 with grinning. However, the weak value for the cat with grinning in the box 2 becomes

$$(\sigma_z \otimes \Pi_2)_w = 0. \tag{2.36}$$

In contrast, the grin is in box 1,

$$(\sigma_z \otimes \Pi_1)_w = 1. \tag{2.37}$$

Thus, the cat is in the box 2, but the grin is in the box 1. Experimentally, Denkmayr et al. confirmed that the spin nature is separated from the neutron [25].

2.3 Reconstructed trajectories based on the de Broglie-Bohm theory

Because of the uncertainty principle, we cannot define the trajectory for the quantum particle. In the double-slit experiment, which path the particle takes is the particle nature, while

the interference pattern on the screen is the wave nature. The wave-particle nature is not measured simultaneously by the complementarity. Despite it, Kocsis et al. reconstructed the trajectories in the double-slit experiment by using the momentum weak value [8] as expected by the de Broglie-Bohm theory [9, 10, 11, 12].

The de Broglie-Bohm theory is one of the most successful examples of the hidden variable theory. In the de Broglie-Bohm theory [10, 11], the velocity of the particle is defined by

$$\dot{\mathbf{x}} \equiv \frac{\mathbf{j}(\mathbf{x},t)}{P(\mathbf{x},t)}, \tag{2.38}$$

$$\mathbf{j}(\mathbf{x},t) = \frac{\hbar}{2m\mathrm{i}}(\phi^*(\mathbf{x},t)\nabla\phi(\mathbf{x},t) - (\nabla\phi^*(\mathbf{x},t))\phi(\mathbf{x},t)), \tag{2.39}$$

$$P(\mathbf{x},t) = \phi^*(\mathbf{x},t)\phi(\mathbf{x},t), \tag{2.40}$$

where $\mathbf{j}(\mathbf{x},t)$ is the probability current and $P(\mathbf{x},t)$ is the probability. The probability and the probability current satisfy the conservation equation

$$\frac{\partial P(\mathbf{x},t)}{\partial t} + \nabla\cdot\mathbf{j}(\mathbf{x},t) = 0. \tag{2.41}$$

All physical processes are described by the particle nature, and the notion of the particle obeys what is called "quantum potential". From (2.38), it is easily shown that the velocity can be written in terms of the momentum weak value [9],

$$\dot{\mathbf{x}} = \frac{1}{m}\mathrm{Re}\,\mathbf{p}_w(\mathbf{x},t) = \frac{1}{m}\mathrm{Re}\left[\frac{\langle\mathbf{x}|\mathbf{p}|\phi(t)\rangle}{\langle\mathbf{x}|\phi(t)\rangle}\right]. \tag{2.42}$$

By solving differential equation (2.42), one can obtain the trajectories without disturbing the interference pattern. Kocsis et al. implemented (2.42) for the double-slit experiment by using photons. The measurement apparatus is prepared as shown in Fig. 2.5. To measure the momentum weak value, the polarization state has been exploited as a probe system. Initially, the probe system (the polarization state) is prepared by

$$|D\rangle = \frac{1}{\sqrt{2}}\left(|H\rangle + |V\rangle\right). \tag{2.43}$$

Then, the weak measurement is performed by a piece of calcite which rotates the polarization state to

$$|D\rangle \to |\Phi\rangle := \frac{1}{\sqrt{2}}\left(\mathrm{e}^{-\mathrm{i}\frac{1}{2}\varphi_k}|H\rangle + \mathrm{e}^{\mathrm{i}\frac{1}{2}\varphi_k}|V\rangle\right), \tag{2.44}$$

where the birefringent phase shift φ_k can be approximated to

$$\varphi_k = \xi\frac{k_x}{|\mathbf{k}|} + \varphi_0, \tag{2.45}$$

where ξ is the coupling strength between the phase for the polarization state and the momentum (wave-number) in the x-direction, k_x. The calcite is tilted to tune $\varphi_0 = 0$ modulo 2π.

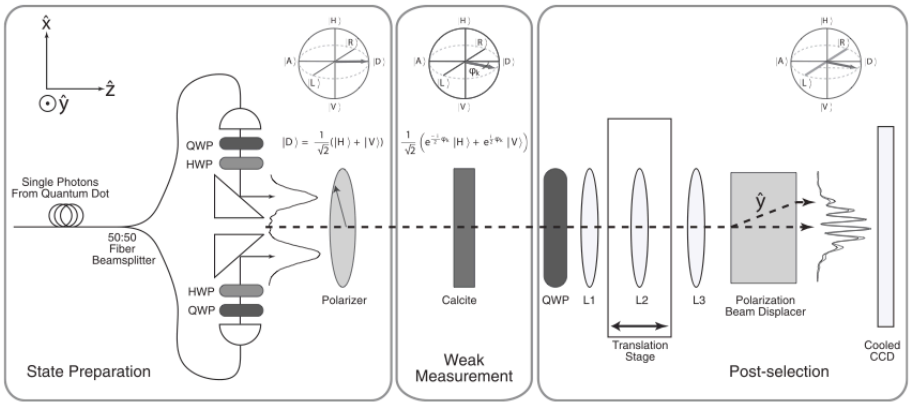

Figure 2.5: Fig. 1 from [8]. The apparatus to reconstruct the trajectories. Single photons are split into two parts on a beam splitter, which represents the double-slit. Then, the polarizer prepares the photons with a polarization $|D\rangle = (|H\rangle + |V\rangle)/\sqrt{2}$. The weak measurement is performed by a piece of calcite which rotates the polarization state to $\left(\mathrm{e}^{-\mathrm{i}\frac{1}{2}\phi_k}|H\rangle + \mathrm{e}^{\mathrm{i}\frac{1}{2}\phi_k}|V\rangle\right)/\sqrt{2}$. Lenses L1, L2, and L3 allow us to measure the image plane with various different distance. A polarization beam displacer is used to measure the polarization of the photons in the basis $|R\rangle, |L\rangle$. A cooled CCD measures the final position of the photons.

The lenses allow us to measure the image plane with arbitrary different distance. Before post-selecting the position of the photons in the x-direction, by using a polarization beam displacer, the polarization state with $|L\rangle = (|H\rangle + \mathrm{i}|V\rangle)/\sqrt{2}$ is displaced 2mm in the y-direction while the polarization state with $|R\rangle = (|H\rangle - \mathrm{i}|V\rangle)/\sqrt{2}$ does not change. Finally, the photons are observed on the cooled CCD (post-selection). The intensities I_R and I_L at the screen for each polarization state are

$$I_R = |\langle\Phi|R\rangle|^2 = \sin^2\left(\frac{\varphi_k}{2} + \frac{\pi}{4}\right) = \frac{1 - \cos\left(\varphi_k + \frac{\pi}{2}\right)}{2} = \frac{1 + \sin\left(\varphi_k\right)}{2}, \tag{2.46}$$

$$I_L = |\langle\Phi|L\rangle|^2 = \cos^2\left(\frac{\varphi_k}{2} + \frac{\pi}{4}\right) = \frac{1 + \cos\left(\varphi_k + \frac{\pi}{2}\right)}{2} = \frac{1 - \sin\left(\varphi_k\right)}{2}. \tag{2.47}$$

From (2.45), we can write the wave number in the x-direction as

$$\frac{k_x}{|\mathbf{k}|} = \frac{1}{\xi}\left(\sin^{-1}\left(\frac{I_R - I_L}{I_R + I_L}\right) - \varphi_0\right), \tag{2.48}$$

where φ_0 equals 0 modulo 2π. The momentum weak value is measured from (2.48), and Kocsis et al. reconstructed the trajectories by (2.42). This reconstructed trajectories coincide with the trajectories predicted by the de Broglie-Bohm theory: see Fig. 2.6.

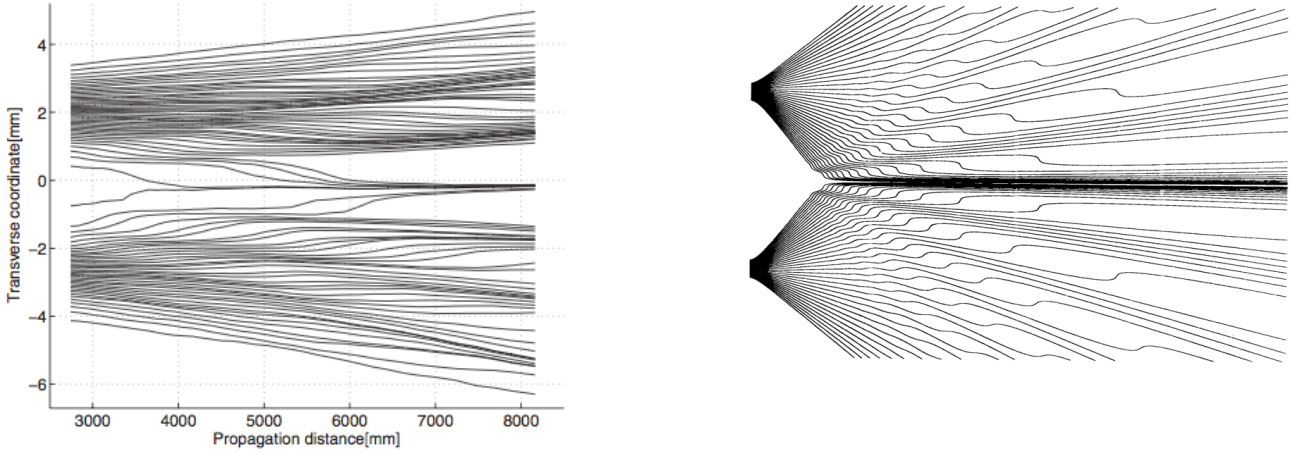

Figure 2.6: Left: Fig.3 from [8]. Trajectories reconstructed of single photons. Right: Fig. 3 from [12]. Predicted trajectories from the de Broglie-Bohm theory in the double-slit experiment.

2.4 Weak measurement

So far we have reviewed several applications of the weak value. In this section we explain the weak measurement and the interpretation of the weak value [27]. Then, we briefly review the definition of the element of reality of Vaidman [28].

Indirect quantum measurement was implemented to measure the weak value in which the object and the meter systems are prepared. The initial state is the product state of the meter and the object systems:

$$\rho := |\Phi\rangle\langle\Phi| \otimes \rho_s, \tag{2.49}$$

$$\rho_s := |\phi\rangle\langle\phi|. \tag{2.50}$$

The meter and the object states ρ evolve under the unitary operator U_w, and the object system becomes entangled with the meter system. The unitary operator is

$$U_w := \exp\left[-\mathrm{i}\frac{g}{\hbar}p \otimes A\right], \tag{2.51}$$

where g, p, and A are a coupling constant, the momentum of the meter system, and the observable on the object system, respectively. Subsequently measuring a particular meter position is equivalent to performing an operation $\mathcal{M}_x$ on a reduced system state,

$$\mathcal{M}_x(\rho_s) = \mathrm{Tr}_d[(|x\rangle\langle x| \otimes \mathbb{I}_s)U_w\rho U_w^\dagger] = M_x\rho_s M_x^\dagger, \tag{2.52}$$

$$M_x = \langle x|U_w|\Phi\rangle, \tag{2.53}$$

where $\mathrm{Tr}_d(\cdot)$ is a partial trace on the meter Hilbert space and M_x is a Kraus operator. Also, we can measure a particular meter momentum p and is equivalent to performing an operation

$\mathcal{N}_p$ on a reduced system state,

$$\mathcal{N}_p(\rho_s) = \mathrm{Tr}_d[(|p\rangle\langle p| \otimes \mathbb{I}_s) U_T \rho U_T^\dagger] = N_p \rho_s N_p^\dagger, \tag{2.54}$$

$$N_p = \langle p|U_w|\Phi\rangle = \exp\left(\frac{gp}{i\hbar}A\right)\langle p|\Phi\rangle, \tag{2.55}$$

where the Kraus operator N_p contains a purely unitary factor A that disturbs the system.

To post-select the object system, the experimenter has to select the outcome of the second measurement for the object system after the interaction U_w. In other words, the experimenter selects the outcome that satisfies a constraint. If we represent the second measurement as a set of projection operators $\{\Pi_f\}$ with parameter f, the total joint probabilities to obtain the sets of measurement results (x, f) and (p, f) are

$$P(x, f) = \mathrm{Tr}_s[\Pi_f \mathcal{M}_x(\rho_s)], \tag{2.56}$$

$$P(p, f) = \mathrm{Tr}_s[\Pi_f \mathcal{N}_p(\rho_s)]. \tag{2.57}$$

The conditional probabilities that we get the result f for the second measurement are defined as

$$P(x|f) = \frac{P(x,f)}{P(f)} = \frac{\mathrm{Tr}_s[\Pi_f \mathcal{M}_x(\rho_s)]}{\mathrm{Tr}_s[\Pi_f \mathcal{E}(\rho_s)]}, \tag{2.58}$$

$$P(p|f) = \frac{P(p,f)}{P(f)} = \frac{\mathrm{Tr}_s[\Pi_f \mathcal{N}_p(\rho_s)]}{\mathrm{Tr}_s[\Pi_f \mathcal{E}(\rho_s)]}, \tag{2.59}$$

$$\mathcal{E}(\rho_s) = \mathrm{Tr}_d[U_w(|\Phi\rangle\langle\Phi| \otimes \rho_s)U_w^\dagger]. \tag{2.60}$$

To obtain the conditional average for the meter position and momentum, we average (2.58) and (2.59) over x and p, respectively,

$${}_f\langle x\rangle_T = \int_{-\infty}^{\infty} dx\, x\, P(x|f) = \frac{\mathrm{Tr}_s[\Pi_f \mathcal{X}_T(\rho_s)]}{\mathrm{Tr}_s[\Pi_f \mathcal{E}(\rho_s)]}, \tag{2.61}$$

$${}_f\langle p\rangle_T = \int_{-\infty}^{\infty} dp\, p\, P(p|f) = \frac{\mathrm{Tr}_s[\Pi_f \mathcal{P}_T(\rho_s)]}{\mathrm{Tr}_s[\Pi_f \mathcal{E}(\rho_s)]}, \tag{2.62}$$

$$\mathcal{X}_T(\rho_s) = \mathrm{Tr}_d[(x \otimes \mathbb{I}_s)U_w(|\Phi\rangle\langle\Phi| \otimes \rho_s)U_w^\dagger], \tag{2.63}$$

$$\mathcal{P}_T(\rho_s) = \mathrm{Tr}_d[(p \otimes \mathbb{I}_s)U_w(|\Phi\rangle\langle\Phi| \otimes \rho_s)U_w^\dagger]. \tag{2.64}$$

To interpret (2.63) and (2.64), we use the canonical commutation relation,

$$\mathcal{X}_T(\rho_i) = \mathcal{X}(\rho_s) + g\mathcal{E}(\{A, \rho_i\}/2), \tag{2.65}$$

$$\mathcal{P}_T(\rho_i) = \mathcal{P}(\rho_i), \tag{2.66}$$

where

$$\mathcal{X}(\rho_s) = \mathrm{Tr}_d[U_w(\{x, |\Phi\rangle\langle\Phi|\}/2 \otimes \rho_s)U_w^\dagger], \tag{2.67}$$

$$\mathcal{P}(\rho_s) = \mathrm{Tr}_d[U_w(\{p, |\Phi\rangle\langle\Phi|\}/2 \otimes \rho_s)U_w^\dagger]. \tag{2.68}$$

When the post-selection is an identity operator $\Pi_f = \mathbb{I}_s$, the unitary operator U_w is canceled in (2.61) and (2.62) because of its cyclic property of total trace,

$$
\begin{aligned}
{}_f\langle x\rangle_T &= \langle x\rangle_0 + g\langle A\rangle_0, && (2.69)\\
{}_f\langle p\rangle_T &= \langle p\rangle_0, && (2.70)
\end{aligned}
$$

where $\langle\cdot\rangle_0$ denotes the expectation value. The average shift from the initial meter position is the expectation value of A. However, there is no shift in the momentum p because the unitary operator U_w and the momentum p commute $[U_w, p] = 0$. Thus, the meter momentum p does not contain information of A.

From the canonical commutation relation, we obtain the final exact expressions of (2.61) and (2.62) as

$$
\begin{aligned}
{}_f\langle x\rangle_T &= \frac{\mathrm{Tr}_s[\Pi_f \mathcal{X}\rho_s]}{\mathrm{Tr}_s[\Pi_f \mathcal{E}(\rho_s)]} + g\frac{\mathrm{Tr}_s[\Pi_f \mathcal{E}(\{A,\rho_s\})]}{2\mathrm{Tr}_s[\Pi_f \mathcal{E}(\rho_s)]}, && (2.71)\\
{}_f\langle p\rangle_T &= \frac{\mathrm{Tr}_s[\Pi_f \mathcal{P}(\rho_s)]}{\mathrm{Tr}_s[\Pi_f \mathcal{E}(\rho_s)]}. && (2.72)
\end{aligned}
$$

Then we expand (2.71) and (2.72) perturbatively with respect to the coupling strength g as

$$
\begin{aligned}
\mathcal{E}(\rho_s) &= \sum_{n=0} \frac{1}{n!}\left(\frac{g}{i\hbar}\right)^n \langle p^n\rangle_0 (\mathrm{ad}\, A)^n(\rho_s), && (2.73)\\
\mathcal{X}(\rho_s) &= \sum_{n=0} \frac{1}{n!}\left(\frac{g}{i\hbar}\right)^n \frac{\langle\{p^n, x\}\rangle_0}{2} (\mathrm{ad}\, A)^n(\rho_s), && (2.74)\\
\mathcal{P}(\rho_s) &= \sum_{n=0} \frac{1}{n!}\left(\frac{g}{i\hbar}\right)^n \langle p^{n+1}\rangle_0 (\mathrm{ad}\, A)^n(\rho_s), && (2.75)
\end{aligned}
$$

where the operation $(\mathrm{ad}A)(\cdot) = [A, \cdot]$ is left-hand action of A in the adjoint representation of its Lie algebra and indicates disturbance of the measurement of the operator A. Ignoring the second oder in g, one obtains

$$
\begin{aligned}
{}_f\langle x\rangle_T &\to \langle x\rangle_0 + \frac{g}{i\hbar}\frac{\langle\{p,x\}\rangle_0}{2}\frac{\mathrm{Tr}_s[\Pi_f(\mathrm{ad}\, A)(\rho_s)]}{\mathrm{Tr}_s(\Pi_f\rho_s)} + g\frac{\mathrm{Tr}_s(\Pi_f\{A,\rho_s\})}{2\mathrm{Tr}_s(\Pi_f\rho_s)}, && (2.76)\\
{}_f\langle p\rangle_T &\to \langle p\rangle_0 + \frac{g}{i\hbar}\langle p^2\rangle_0 \frac{\mathrm{Tr}_s[\Pi_f(\mathrm{ad}\, A)(\rho_s)]}{\mathrm{Tr}_s(\Pi_f\rho_s)}. && (2.77)
\end{aligned}
$$

Introducing complex valued weak values, we rewrite (2.76) and (2.77) as

$$
\begin{aligned}
{}_f\langle x\rangle_T &= \langle x\rangle_0 + \frac{g}{\hbar}\frac{\langle\{p,x\}\rangle_0}{2}(2\mathrm{Im}A_w) + g\mathrm{Re}A_w, && (2.78)\\
{}_f\langle p\rangle_T &= \langle p\rangle_0 + \frac{g}{\hbar}\langle p^2\rangle_0 (2\mathrm{Im}A_w), && (2.79)
\end{aligned}
$$

where $A_w = \mathrm{Tr}_s(\Pi_f A\rho_s)/\mathrm{Tr}_s(\Pi_f\rho_s)$. If the wave function $\Phi(x)$ is purely real, so that the measurement is minimally disturbing, then $\langle\{p,x\}/2\rangle_0$ vanishes,

$$
\begin{aligned}
\langle\{p,x\}\rangle_0 &= \int dx \Phi^*(x)\{x,p\}\Phi(x)\\
&= -\mathrm{i}\hbar\int dx \Phi^*(x)\left(2x\Phi'(x) + \Phi(x)\right), && (2.80)
\end{aligned}
$$

because (2.80) is purely imaginary despite the real valuedness of the expectation value $\langle\{p,x\}\rangle_0$, so that the integral must be zero. $\{x,p\}$ is Hermite, and hence (2.80) must be real.

According to (2.78) and (2.79), the shift from the initial meters represents the real and the imaginary parts of the weak values. Let us briefly review the conclusion by Dressel et al. [27]. ReA_w gives directly the conditioned shift of the weak value A_w. Since the disturbance is indicated by ad$A$, there is no further perturbation of the measurement in (2.76) if the meter state $\Phi(x)$ is a real number. Thus, ReA_w is a conditioned average of A in the ideal limit. In contrast, Im A_w in (2.79) can be regarded as the disturbance of the measurement which is indicated by ad$A$ in (2.77). As we have seen in (2.79), the imaginary part of the weak value ImA_w is described by ad$A$, which can be written as

$$\delta_A(\cdot) = -\mathrm{i}(\mathrm{ad}A)(\cdot), \tag{2.81}$$

from which the total probability $P(f)$ can be changed by ϵ,

$$P_\epsilon(f) = \mathrm{Tr}_s[\Pi_f \exp(\epsilon\delta_A)(\rho_s)], \tag{2.82}$$

where $\exp(\epsilon\delta_A)(\rho_s) = \exp(-\mathrm{i}\epsilon A)\rho_s \exp(\mathrm{i}\epsilon A)$. Then, Im$A_w$ can be derived from the directional derivative operation,

$$2\mathrm{Im}A_w = \frac{\partial}{\partial\epsilon} \ln P_\epsilon(f)\Big|_{\epsilon=0}. \tag{2.83}$$

Dressel et al. pointed out that

> *the imaginary part of the weak value is half the logarithmic directional derivative of the postselection probability along the natural unitary flow generated by A* [27].

Also, Dressel et al. claimed that the imaginary part of the weak value does not contain any information about the measurement of A, but the disturbance of the weak measurement.

2.4.1 An element of reality

In this subsection, we briefly introduce the interpretation of the weak value discussed by Vaidman based on the element of reality [28]. An element of reality is originally proposed by Einstein, Podolsky, and Rosen [32]. The EPR definition of the element of reality is:

> *If, without in any way disturbing the system, we can predict with certainty(i.e. with probability equal to unity) the value of a physical quantity, then there exists an element of physical reality corresponding to this physical quantity* [32].

The phrase "without in any way disturbing the system" implies that the non-existence of a space-like separated interaction. Bell showed, however, that this type of element of reality is not consistent [33].

Redhead proposed a different type of the element of reality:

If we can predict with certainty, or at any rate with probability one, the result of measuring a physical quantity at time t, then, at time t, there exists an element of reality corresponding to this physical quantity and having value equal to the predicted measurement result [34].

The definition introduced by Redhead does not mention that the value is measured while, in EPR definition, the value is measured. In this definition proposed by Redhead, when an EPR pair of spin-1/2 particles is considered, we cannot state that there are any element of reality because we cannot predict the outcome of the measurement.

Let us briefly introduce the definition of the reality given by Vaidman. The initial meter state is assumed to be

$$\langle x|\Phi\rangle = \Phi(x) = (\Delta^2\pi)^{-1/4}\mathrm{e}^{-x^2/2\Delta^2}, \tag{2.84}$$

where Δ represents the width of the Gaussian distribution. If the initial state of the object system is an eigenstate of the observable A, $|\Phi\rangle = |a_i\rangle$, then Eq. (2.56) gives the joint probability $P(x, f)$ as

$$P(x, f) = (\Delta^2\pi)^{-1/2}\mathrm{e}^{-(x-g\,a_i)^2/\Delta^2}, \tag{2.85}$$

where we assumed $\Pi_f = \mathbb{I}_s$. a_i is the eigenvalue of the observable A. The probability distribution does not change its shape after the measurement, but the shift of the position. The eigenvalue a_i is considered to be the element of reality. Vaidman suggested to take into account this property for the definition:

If we are certain that a procedure for measuring a certain variable will lead to a definite shift of the unchanged probability distribution of the pointer, then there is an element of reality: the variable equal to this shift [28].

The ideal measurement yields the shift of the eigenvalue for an ensemble even if the meter state has a width Δ. However, if the initial state of the object system is a general state $|\Phi\rangle = \sum \alpha_i|a_i\rangle$, then the joint probability $P(x, f)$

$$P(x, f) = (\Delta^2\pi)^{-1/2}\sum_i |\alpha_i|^2\mathrm{e}^{-(x-g\,a_i)^2/\Delta^2}, \tag{2.86}$$

changes its shape not only its position. The element of reality is recovered if we add a "collapse" to one of its eigenstate. This is the definition done by Bohr for the element of reality. However, the element of reality can be obtained after the measurement.

Aharonov et al. proposed new procedure to measure the physical value, instead of taking a very small value of Δ (which will lead to the strong measurement), by assuming that the uncertainty in P is small so that the object system may not change during the measurement. In this case, the interaction is very small, and hence this procedure is called the weak measurement. The element of reality can be observed when the weak measurement is considered.

In the weak measurement, we assume $\Delta/g \gg a_i$ for all eigenvalues a_i. We can expand (2.86) around $Q = 0$ as

$$\begin{aligned} P(x,f) &= (\Delta^2\pi)^{-1/2}\sum |\alpha_i|^2 \mathrm{e}^{-(x-g\,a_i)^2/\Delta^2} \simeq (\Delta^2\pi)^{-1/2}\sum |\alpha_i|^2(1-(x-g\,a_i)^2/\Delta^2) \\ &\simeq (\Delta^2\pi)^{-1/2}\mathrm{e}^{-(x-g\sum|\alpha_i|^2 a_i)^2/\Delta^2}, \end{aligned} \tag{2.87}$$

which does not change the shape of the probability but shift its position, and the shift is equal to the expectation value $\sum |\alpha_i|^2 a_i$. According to Vaidman's definition, the average value $\sum |\alpha_i|^2 a_i$ is the element of reality.

So far, the post-selection of the object system has not been considered. The post-selection is described by $\Pi_f = |\psi\rangle\langle\psi|$. When we take into account the effect of the post-selection, the shift in the distribution probability is equal to the real part of the weak value of the observable A:

$$A_w = \frac{\langle\psi|A|\phi\rangle}{\langle\psi|\phi\rangle} = \sum_i \alpha_i a_i \frac{\langle\psi|a_i\rangle}{\langle\psi|\phi\rangle}. \tag{2.88}$$

Let us show that the shift in $P(x,f)$ coincides with the real part of the weak value Re A_w,

$$\begin{aligned} P(x,f) &= \sum_{i,j} \alpha_i\alpha_j^*(\Delta^2\pi)^{-1/2}\exp\left(-(x-g\,a_i)^2/2\Delta^2\right)\exp\left(-(x-g\,a_j)^2/2\Delta^2\right)\langle\psi|a_i\rangle\langle a_j|\psi\rangle \\ &\simeq \sum_{i,j} \alpha_i\alpha_j^*(\Delta^2\pi)^{-1/2}\left(1-\frac{x^2-g\,a_i\,x-g\,a_j\,x}{\Delta^2}\right)\langle\psi|a_i\rangle\langle a_j|\psi\rangle \\ &\simeq |\langle\psi|\phi\rangle|^2(\Delta^2\pi)^{-1/2}\left(1-\frac{(x-2g\,\mathrm{Re}\,A_w)^2}{\Delta^2}\right) \\ &\simeq |\langle\psi|\phi\rangle|^2(\Delta^2\pi)^{-1/2}\exp\left(-\frac{(x-2g\,\mathrm{Re}\,A_w)^2}{\Delta^2}\right). \end{aligned} \tag{2.89}$$

We can deduce the imaginary part of the weak value as well by changing the representation of the initial meter state,

$$\langle p|\Phi\rangle = \Phi(p) = \left(\frac{\Delta^2}{\hbar^2\pi}\right)^{1/4}\mathrm{e}^{-p^2\Delta^2/\hbar^2}. \tag{2.90}$$

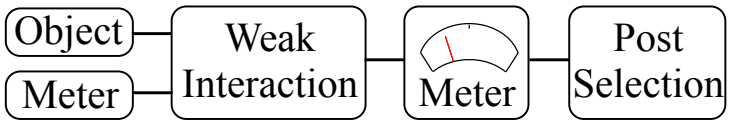

Figure 2.7: The outline of the weak measurement. Firstly, we prepare the object and the meter systems, let them weakly interact, measure the meter state, and finally post-select the object state.

Then, the imaginary part of the weak value Im A_w can be observed by the shift of the distribution probability,

$$\begin{aligned} P(p,f) &= \sum_{i,j} \alpha_i \alpha_j^* \left(\frac{\Delta^2}{\hbar^2\pi}\right)^{1/2} \exp\left(-p^2\Delta^2/\hbar^2 - \mathrm{i}\, g\, p\, a_i + \mathrm{i}\, g\, p\, a_j\right) \langle\psi|a_i\rangle\langle a_j|\psi\rangle \\ &\simeq \sum_{i,j} \alpha_i \alpha_j^* \left(\frac{\Delta^2}{\hbar^2\pi}\right)^{1/2} \mathrm{e}^{-p^2\Delta^2/\hbar^2} \left(1 - \mathrm{i}\, g\, p\, a_i + \mathrm{i}\, g\, p\, a_j\right) \langle\psi|a_i\rangle\langle a_j|\psi\rangle \\ &= |\langle\psi|\phi\rangle|^2 \left(\frac{\Delta^2}{\hbar^2\pi}\right)^{1/2} \mathrm{e}^{-p^2\Delta^2/\hbar^2} \left(1 - 2gp\mathrm{Im}\, A_w\right) \\ &\simeq |\langle\psi|\phi\rangle|^2 \left(\frac{\Delta^2}{\hbar^2\pi}\right)^{1/2} \exp\left(-p^2\Delta^2/\hbar^2 - 2gp\mathrm{Im}\, A_w\right) \\ &\simeq |\langle\psi|\phi\rangle|^2 \left(\frac{\Delta^2}{\hbar^2\pi}\right)^{1/2} \exp\left(-\frac{\Delta^2}{\hbar^2}\left(p - \frac{g\hbar}{\Delta}\mathrm{Im}\, A_w\right)^2\right). \end{aligned} \tag{2.91}$$

Thus, the real and the imaginary parts of the weak values can be obtained from the shift in the distribution probabilities, and hence the weak value can be regarded as an element of reality.

2.5 Weak measurement with the spin state

In this section we consider the time-dependent weak value of the projection operator Π_A. The protocol of weak measurement can be described by Fig. 2.7. We prepare the product state of the object and the meter states, make the product state entangle by weak interaction, and then measure the spin state (the meter state). After the measurement of the spin state, one singles out the events which successfully post-selects the object system.

We begin by considering the initial state (pre-selected state) $|\phi\rangle$ at $t = 0$ and the final state (post-selected state) $|\psi\rangle$ at $t = T$. The pre-selected state $|\phi\rangle$ evolves under the unitary evolution $U(t) = \exp(-\mathrm{i}Ht/\hbar)$: $|\phi(t)\rangle = U(t)|\phi\rangle$. We assume that the measurement is performed at time t. We may regard that the post-selected state evolves backward in time: $|\psi(T-t)\rangle = U^\dagger(T-t)|\psi\rangle$. As a meter system, we exploit a spin-1/2 state $|s_i\rangle$ [35, 16], and

suppose that the spin state $|s_i\rangle$ does not evolve other than under the weak measurement. The composite system of the meter and object is initially in the state

$$\begin{aligned} \rho &= |s_i\rangle\langle s_i| \otimes |\phi\rangle\langle\phi| && (2.92)\\ &= |s_i\rangle\langle s_i| \otimes \rho_s, && (2.93) \end{aligned}$$

and evolves under $U(t)$ until the weak measurement has been performed,

$$\begin{aligned} \rho(t) &= |s_i\rangle\langle s_i| \otimes U(t)|\phi\rangle\langle\phi|U^\dagger(t) && (2.94)\\ &= |s_i\rangle\langle s_i| \otimes |\phi(t)\rangle\langle\phi(t)| && (2.95)\\ &= |s_i\rangle\langle s_i| \otimes \rho_s(t), && (2.96) \end{aligned}$$

where $\rho_s(t) = |\phi(t)\rangle\langle\phi(t)|$. We describe the weak measurement as

$$U_w := \exp\left[-\mathrm{i}g\sigma_y \otimes \Pi_A\right], \tag{2.97}$$

where g is a coupling constant and Π_A satisfies the condition, $\Pi_A^2 = \Pi_A$. We denote the Pauli matrices as σ_x, σ_y, and σ_z.

The measurements of the meter system are performed for σ_x and σ_y as described by

$$\begin{aligned} \mathcal{M}_{\sigma_x}(\rho_s(t)) &= \mathrm{Tr}_d\left[(|\sigma_x\rangle\langle\sigma_x| \otimes \mathbb{I}_s)U_w\rho(t)U_w^\dagger\right], && (2.98)\\ \mathcal{N}_{\sigma_y}(\rho_s(t)) &= \mathrm{Tr}_d\left[(|\sigma_y\rangle\langle\sigma_y| \otimes \mathbb{I}_s)U_w\rho(t)U_w^\dagger\right]. && (2.99) \end{aligned}$$

After the measurement for the meter system, the object system is post-selected at time T, and the joint probability that the post-selection is successfull is given by

$$\begin{aligned} P(\sigma_x, f) &= \mathrm{Tr}_s\left[\Pi_f\mathcal{M}_{\sigma_x}(\rho_s(t))\right], && (2.100)\\ P(\sigma_y, f) &= \mathrm{Tr}_s\left[\Pi_f\mathcal{N}_{\sigma_y}(\rho_s(t))\right], && (2.101) \end{aligned}$$

where $\Pi_f = U^\dagger(T-t)|\psi\rangle\langle\psi|U(T-t) = |\psi(T-t)\rangle\langle\psi(T-t)|$. The total probability for obtaining the post-selection readout f is also written as

$$P(f) = \mathrm{Tr}_s\left[\Pi_f\mathrm{Tr}_d\left[U_w\rho(t)U_w^\dagger\right]\right], \tag{2.102}$$

and then the conditional probability is defined as

$$\begin{aligned} P(\sigma_x|f) &= \frac{P(\sigma_x, f)}{P(f)}, && (2.103)\\ P(\sigma_y|f) &= \frac{P(\sigma_y, f)}{P(f)}. && (2.104) \end{aligned}$$

For the eigenvalue 1 of σ_x, the conditional probability $P(\sigma_x, f)$ is

$$P(\sigma_x = +1, f) = \frac{1}{2}|\langle\psi(t-t)|\phi(t)\rangle + (\sin g + \cos g - 1)\langle\psi(T-t)|\Pi_A|\phi(t)\rangle|^2, \tag{2.105}$$

where we have assumed that $|s_i\rangle$ is the spin-down eigenstate of σ_z. Detailed calculations are in Appendix A. Similarly, we get the conditional probabilities,

$$P(\sigma_x = -1, f) = \frac{1}{2}|\langle\psi(T-t)|\phi(t)\rangle + (-\sin g + \cos g - 1)\langle\psi(T-t)|\Pi_A|\phi(t)\rangle|^2, \tag{2.106}$$

$$P(\sigma_y = 1, f) = \frac{1}{2}|\langle\psi(T-t)|\phi(t)\rangle + (-1 + \mathrm{e}^{\mathrm{i}g})\langle\psi(T-t)|\Pi_A|\phi(t)\rangle|^2, \tag{2.107}$$

$$P(\sigma_y = -1, f) = \frac{1}{2}|\langle\psi(T-t)|\phi(t)\rangle + (-1 + \mathrm{e}^{-\mathrm{i}g})\langle\psi(T-t)|\Pi_A|\phi(t)\rangle|^2. \tag{2.108}$$

From these probabilities, we can see how the initial object state is disturbed by the weak measurement dependent on the coupling constant g. The total probability $P(f)$ for obtaining the post-selection result f is

$$P(f) = \sum_{\sigma_x=\pm1} P(\sigma_x, f) = \sum_{\sigma_y=\pm1} P(\sigma_y, f) \tag{2.109}$$

$$\begin{aligned} &= |\langle\psi(T-t)|\phi(t)\rangle|^2 + 2(1-\cos g)|\langle\psi(T-t)|\Pi_A|\phi(t)\rangle|^2 \\ &\quad +2(-1+\cos g)\mathrm{Re}\left[\langle\phi(t)|\psi(T-t)\rangle\langle\psi(T-t)|\Pi_A|\phi(t)\rangle\right]. \end{aligned} \tag{2.110}$$

In the weak limit $g \to 0$, the expectation value at the meter can be written as

$$\begin{aligned} \langle\sigma_x\rangle_d &= \sum_{\sigma_x=\pm1} \sigma_x P(\sigma_x|f) \\ &\simeq \frac{2\sin g\mathrm{Re}\left[\langle\phi(t)|\psi(T-t)\rangle\langle\psi(T-t)|\Pi_A|\phi(t)\rangle\right]}{|\langle\psi(T-t)|\phi(t)\rangle|^2} \\ &= 2\sin g\mathrm{Re}\,\Pi_{A_w}(t), \end{aligned} \tag{2.111}$$

$$\begin{aligned} \langle\sigma_y\rangle_d &= \sum_{\sigma_y=\pm1} \sigma_y P(\sigma_y|f) \\ &\simeq \frac{2\sin g\mathrm{Re}\left[\mathrm{i}\langle\phi(t)|\psi(T-t)\rangle\langle\psi(T-t)|\Pi_A|\phi(t)\rangle\right]}{|\langle\psi(T-t)|\phi(t)\rangle|^2} \\ &= -2\sin g\mathrm{Im}\,\Pi_{A_w}(t). \end{aligned} \tag{2.112}$$

$$\Pi_{A_w}(t) = \frac{\langle\psi(T-t)|\Pi_A|\phi(t)\rangle}{\langle\psi(T-t)|\phi(t)\rangle} \tag{2.113}$$

Thus, we can get the real and the imaginary parts of the time-dependent weak values $\Pi_{A_w}(t)$. In general, the weak value is a complex number. Although all physical values must have a real number, weak values may be measured by the weak measurements.

2.5.1 Example

In this subsection, we show how to measure the position weak value by using spin-1/2 state as the meter system [35, 16], and how the measurement weakly disturbs the initial state. The meter state is assumed to be the spin-1/2 down state at time $t = 0$, and the total system is

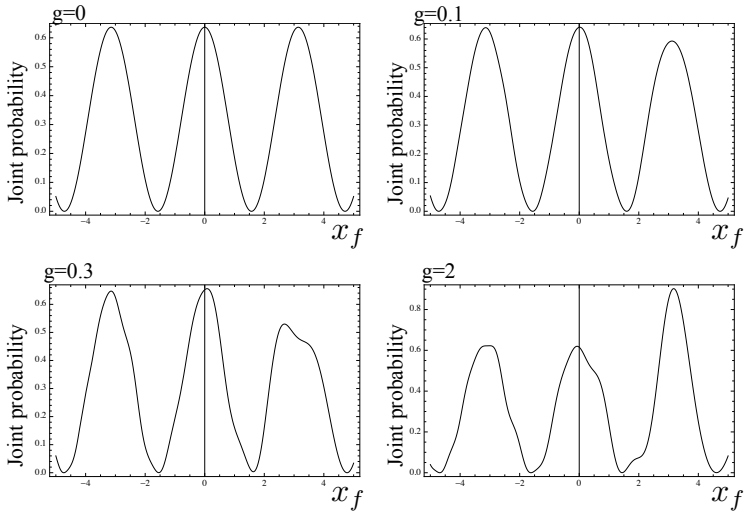

Figure 2.8: The joint probability with $A = \int_{x-\epsilon}^{x+\epsilon} dx\,|x\rangle\langle x|$, $|\phi\rangle = (|x_i\rangle + |-x_i\rangle)/\sqrt{2}$ and $|\psi\rangle = |x_f\rangle$, which we put the parameters as $x_i = T = m = \hbar = T = 1$, $t = \epsilon = 0.5$, and $x = 3$ while changing the coupling constant g. Even if the coupling constant g becomes large, the interference pattern can be seen, being compensated by smallness of ϵ.

written as the product state of the object and the meter states. At an intermediate time t, we rotate the Bloch sphere around the y-axis at a certain position, i.e., creating entanglement between the object and the meter states. The angle of the rotation depends on the pre- and post-selections, not only on the coupling constant g and the operator Π_A. Finally, the expectation value of the meter system with the post-selection is measured (e.g. by the Stern-Gerlach experiment). Then, as we see below, the weak value is obtained.

We begin by putting the projection operator $\Pi_A = \int_{x-\epsilon}^{x+\epsilon} dx\,|x\rangle\langle x|$, where ϵ is supposed to be infinitesimally small because we expect the position of the particle in a tiny region. Naturally, Π_A satisfies $\Pi_A^2 = \Pi_A$. We have shown in (2.111) and (2.112) that the real and imaginary parts of the weak values appear in the meter expectation value in the weak limit $g \to 0$. If ϵ is infinitesimally small, we can approximate $\Pi_A \simeq 2\epsilon|x\rangle\langle x|$, and in this limit the coupling constant g is not necessarily small as we have derived in (2.111) and (2.112). The weakness is compensated by the smallness of ϵ. Thus, by assuming that ϵ is infinitesimally small (the coupling constant g is not necessarily small), we obtain

$$\begin{aligned}
\langle\sigma_x\rangle_d &= \sum_{\sigma_x=\pm} \sigma_x P(\sigma_x|f), \\
&\simeq 4\epsilon \sin g \mathrm{Re}\,\Pi_{xw}(t), \qquad (2.114) \\
\langle\sigma_y\rangle_d &= \sum_{\sigma_y=\pm} \sigma_y P(\sigma_y|f), \\
&\simeq -4\epsilon \sin g \mathrm{Im}\,\Pi_{xw}(t), \qquad (2.115) \\
\Pi_{xw}(t) &= \frac{\langle\psi(T-t)|\Pi_x|\phi(t)\rangle}{\langle\psi(T-t)|\phi(t)\rangle}, \qquad (2.116)
\end{aligned}$$

where $\Pi_x = |x\rangle\langle x|$. If we put the post-selected state as the momentum eigenstate with the momentum zero, $|\psi\rangle = |p = 0\rangle$, the time-dependent wave function $\phi(x,t) = \langle x|\phi(t)\rangle$ except for the total phase can be observed [16]. By integrating $\Pi_{xw}(t)$ over x with the weight x, we have

$$\begin{aligned} x_w(t) &= \frac{\langle\psi(T-t)|x|\phi(t)\rangle}{\langle\psi(T-t)|\phi(t)\rangle} \\ &= \int_{-\infty}^{\infty} dx\, \Pi_{xw}(t)\, x. \end{aligned} \tag{2.117}$$

The basic idea goes as follows: the operator x can be expressed in the basis set $\{|x\rangle\}$, and the weak value $x_w(t)$ is consist with the real value x and the complex conditional probability $\Pi_{xw}(t)$ [36]. Meanwhile, the momentum weak value also can be derived similarly.

Let us evaluate the joint probability $P(\sigma_x = +1, f)$ to know how the weak measurement disturbs the system. Without using any approximation, we can get the exact joint probability for any ϵ and g from (2.105),

$$P(\sigma_x = +1, f) = \frac{1}{2}\left|\langle\psi(t-t)|\phi(t)\rangle + (\sin g + \cos g - 1)\int_{-\epsilon}^{\epsilon} dx\langle\psi(T-t)|x\rangle\langle x|\phi(t)\rangle\right|^2. \tag{2.118}$$

In this paper, as an example, we choose the double-slit thought experiment which is our main interest in the following chapters. As we will see later, the pre- and post-selected states are described as $|\phi\rangle = (|x_i\rangle + |-x_i\rangle)/\sqrt{2}$ and $|\psi\rangle = |x_f\rangle$, respectively. The object system is evolved under the free Hamiltonian $H = p^2/2m$. For simplicity, by putting $x_i = T = m = \hbar = T = 1$, $t = \epsilon = 0.5$, and $x = 3$, we obtain Fig. 2.8, and it is clear that the interference pattern is observed for any coupling constant. We have presumed that ϵ is small compared to x_i. The interference pattern can be seen even if the coupling constant g becomes large: Fig. 2.8.

2.6 Summary

This chapter mainly consists of the weak value and the weak measurement. We have seen several applications of the weak value which allows us to intuitively interpret quantum mechanics. Not only the intuitive interpretation but also the intriguing aspect of the weak value has been taken up by the quantum Cheshire cat [24]. Then, the weak measurement has been introduced and the interpretation of the weak value has been performed.

We have confirmed that the position (momentum) weak value can be obtained by using the spin-1/2 state, and the coupling constant g is not necessarily small if ϵ is small enough, which means that rotation of the angle is performed in the narrow region $x \pm \epsilon$. If the interaction between the object and the meter systems has performed in a small region, then the interaction becomes obviously weak. One may wonder if obtaining the position weak value and the interference pattern simultaneously seems to contradict the complementarity. However, due to the statistical nature of the weak value, the weak measurement does not tell anything about each event. Thus, the position weak value is consistent with quantum mechanics.

Chapter 3

Quantum interference

Quantum interference is one of the most significant aspects of quantum mechanics. To analyze the weak value, we exploit the quantum interference. In this chapter, the relation between the imaginary part of the weak value and the interference effect becomes apparent, and we successfully obtain a physical interpretation of the imaginary part of the weak value. Then, this result is applied to the double-slit experiment, and we show that the connection between the imaginary part of the momentum weak value and interference [29]. As another example, the spin-1/2 system is considered and the importance of the choice of the path is shown.

3.1 General argument

In this section, we show the relation between the weak value and interference. We show that the weak value of A can be obtained from the transition amplitude [26, 27], and then we define the quantum interference from the transition probability by introducing paths between a pre- and post-selected states.

We begin by considering n-dimensional Hilbert space. We choose $|\phi\rangle$ and $|\psi\rangle$ as the pre- and post-selected states, respectively. The definition of the weak value of an observable A is

$$A_w = \frac{\langle\psi|A|\phi\rangle}{\langle\psi|\phi\rangle}. \tag{3.1}$$

Let us consider the transition amplitude,

$$K(\alpha) := \langle\psi|u_A(\alpha)|\phi\rangle, \tag{3.2}$$

which means, between the two states $|\phi\rangle$ and $|\psi\rangle$, intermediately operating the unitary transformation $u_A(\alpha) = \exp[-\mathrm{i}\alpha A]$. $u_A^\dagger(\alpha)|\psi\rangle$ may be regarded as a family of post-selected states. Taking the logarithmic derivative of $K(\alpha)$ with respect to α and taking the limit $\alpha \to 0$, one obtains the weak value A_w,

$$A_w = \mathrm{i}\lim_{\alpha\to 0}\frac{1}{K(\alpha)}\frac{\partial K(\alpha)}{\partial\alpha}. \tag{3.3}$$

In [26, 27], α is regarded as the parameter of the back reaction on the system when the measurement of A is performed. Instead of considering the parameter α as the back reaction of the weak measurement, in this paper we utilize the parameter α to see the variation of the transition probability.

We define the quantum interference by selecting an orthonormal set of states $\{|\chi_k\rangle\}$,

$$\mathbb{I} = \sum_k |\chi_k\rangle\langle\chi_k|. \tag{3.4}$$

Substituting (3.4) to (3.2) and taking the absolute square of the transition amplitude, we have

$$\begin{aligned} |K(\alpha)|^2 &= \left|\sum_k \langle\psi|u_A(\alpha)|\chi_k\rangle\langle\chi_k|\phi\rangle\right|^2 \\ &= \sum_k |K_k(\alpha)|^2 + \sum_{j\neq k} K_k(\alpha)K_j^*(\alpha), \end{aligned} \tag{3.5}$$

where $K_k(\alpha) := \langle\psi|u_A(\alpha)|\chi_k\rangle\langle\chi_k|\phi\rangle$ is the transition amplitude via intermediate state $|\chi_k\rangle$. The first, diagonal, part in (3.5) represents the classical transition probability while the second, off-diagonal, part expresses the interference effect between different paths. The interference is different depending on the choice of the basis. Of course, if the cross terms in (3.5) are independent of α, the interference cannot be observed.

We point out here that whenever the interference pattern is discussed, we implicitly assume the path which causes the interference pattern. Consider that we have the pre-selected state,

$$|\phi\rangle = \int_{-\sigma}^{\sigma} dx\, |x\rangle, \tag{3.6}$$

which describes the slit of a finite width 2σ. The post-selection is the position eigenstate $|x_f\rangle$. The generator of the transformation (the momentum operator p, i.e., $A = p$) is acting on the post-selection. We consider a massive particle which is governed by the free Hamiltonian, $U(T) = \exp(-\mathrm{i}p^2T/2m\hbar)$. The interference pattern is observed (see Fig. 3.1) by regarding the path as

$$K_x(\alpha) = \langle x_f|u_p(\alpha)U(T)|x\rangle. \tag{3.7}$$

Naturally, the interference term (the off-diagonal term in (3.5)) depends on α.

In the same vain, we prepare a Gaussian distribution for the pre-selection,

$$|\phi\rangle = \int_{-\infty}^{\infty} dx \frac{\exp\left(-\frac{x^2}{2\sigma^2}\right)}{(\pi\sigma)^{1/4}}|x\rangle. \tag{3.8}$$

The transition probability is also given by a Gaussian distribution: see Fig. 3.1 from which the interference term again depends on α if the partial path is given by (3.7). Nonetheless, we usually do not regard the transition probability as interference. We regard that the Gaussian

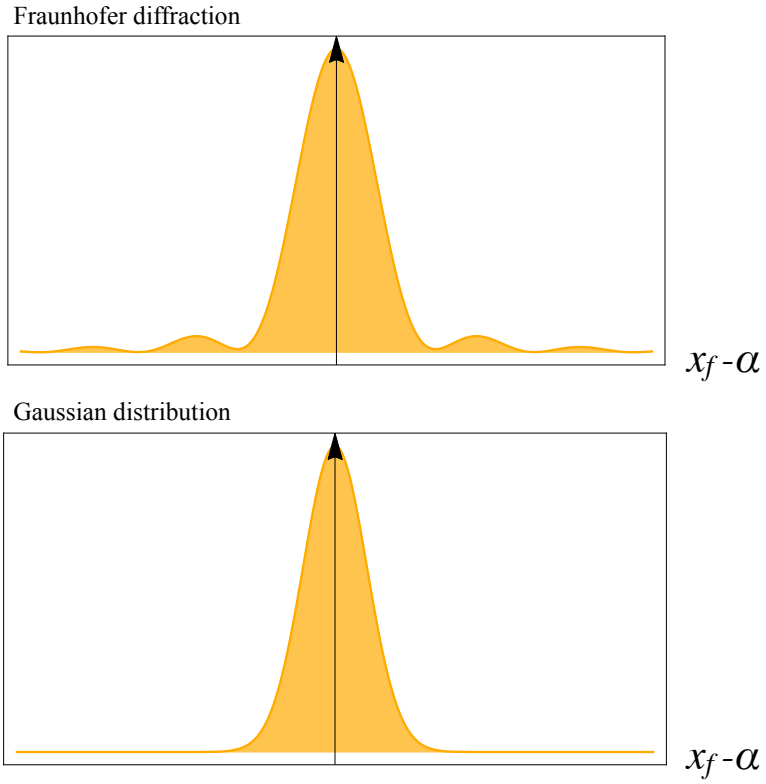

Figure 3.1: Orange filled curve is the transition probability $|K(\alpha)|^2 = |\langle x_f|u_p(\alpha)U(T)|\phi\rangle|^2$. (Above) The transition probability for the pre-selection (3.6) is known as the Fraunhofer diffraction. (Below) The transition probability for the pre-selection (3.8) is expressed by the Gaussian distribution.

distribution of the transition probability is caused by the distribution of the particle not by the interference. Namely, we implicitly assume only one path. Consequently, we assert that the interference effect should depend on the choice of the path.

For each path $K_k(\alpha)$, the weak value A_w^k is derived as (3.3):

$$\begin{aligned} A_w^k &= \frac{\langle\psi|A|\chi_k\rangle}{\langle\psi|\chi_k\rangle} \\ &= \mathrm{i}\lim_{\alpha\to 0}\frac{1}{K_k(\alpha)}\frac{\partial K_k(\alpha)}{\partial\alpha}. \end{aligned} \tag{3.9}$$

To examine the variation of terms in (3.5) with respect to α, we take the logarithmic derivative

of (3.5) and the limit $\alpha \to 0$:

$$\mathcal{I} := \frac{1}{2}\lim_{\alpha\to 0}\frac{1}{|K(\alpha)|^2}\frac{\partial}{\partial\alpha}\left(|K(\alpha)|^2 - \sum_k |K_k(\alpha)|^2\right), \tag{3.10}$$

$$= \mathrm{Im}\left[A_w - \sum_{k=1}^{n} A_w^k P_k\right], \tag{3.11}$$

where $P_k := |K_k(0)|^2/|K(0)|^2$ is the relative probability for the intermediate process k. In general, P_k does not satisfy $\sum_k P_k = 1$. We call $\mathcal{I}$ the index of interference because this index $\mathcal{I}$ is defined by the interference term. The index of interference $\mathcal{I}$ can be expressed as the difference in the imaginary part of the weak value between the total process and the average of the intermediate path with the relative probability P_k. Note that, because we can express the imaginary part of the weak value in terms of the logarithmic derivative of the probability transition $|K(0)|^2$, a tiny value of $|K(0)|^2$ will make the imaginary part of the weak value enormous [29].

Several examples including the double-slit experiment and the spin-1/2 system are discussed in the following sections.

3.2 Double-slit experiment

In this section, as a simple example of the above discussion, we consider the double-slit experiment. We show that the imaginary part of the momentum weak value is proportional to the variation of interference fringes.

The double-slit experiment is expressed by a screen and a sheet with two narrow slits at $S_\pm$. The screen and the sheet are set in parallel to each other at a certain distance as Fig. 3.2. A particle goes through these slits and makes interference fringes on the screen. However, since it is difficult to describe the effect that the particle is passing through these slits, we suppose a superposition of the particle localized around these slits at time $t = 0$. Considering the double-slit experiment, we have to take into account a two-dimensional problem. However, we ignore the y-axis because the axis perpendicular to the screen plays no essential role. The pre-selected state at time $t = 0$ is

$$|\phi\rangle = \frac{|x_i\rangle + |-x_i\rangle}{\sqrt{2}}, \tag{3.12}$$

and the post-selected state at $t = T$ is

$$|\psi\rangle = |x_f\rangle, \tag{3.13}$$

where the post-selected state $|\psi\rangle$ coincides with the measurement at the point x_f. We assume the free Hamiltonian $H = p^2/2m$ where m is the mass of the particle and p is a momentum alongside the x-direction. The pre-selected state evolves under the unitary evolution $U(t) =$

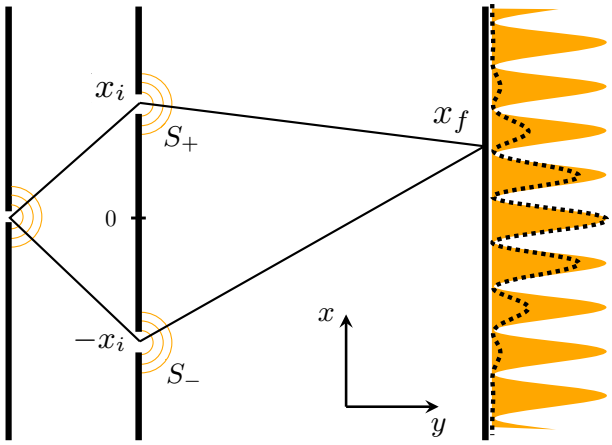

Figure 3.2: The double-slit thought experiment. The particle is localized around $S_\pm$ at time $t = 0$ and arrived at x_f at time $t = T$. This particle cause interference on the screen, and the orange filled curve represents the interference fringes(the transition probability) especially when one choose the superposition of the position eigenstate as the pre-selected state. If one prepare the superposition of the Gaussian state instead of the position eigenstate, the transition probability becomes more realistic and is drawn in the dashed curve.

$\exp[-\mathrm{i}Ht/\hbar]$. The transition probability is derived from the Feynman kernel (propagator) for the free Hamiltonian,

$$\langle x_f|U(T)|x_i\rangle = \sqrt{\frac{m}{2\pi\mathrm{i}\hbar T}}\exp\left(\mathrm{i}\frac{m(x_f-x_i)^2}{2\hbar T}\right), \tag{3.14}$$

and hence the transition probability is

$$|\langle\psi|U(T)|\phi\rangle|^2 = \frac{m}{\pi\hbar T}\cos^2\left(\frac{m}{\hbar}\frac{x_f x_i}{T}\right). \tag{3.15}$$

From the transition probability (3.15), we can derive the condition that the interference pattern becomes constructive. It can be shown that the condition derived from (3.15) coincides with that of Young's double-slit experiment by using the matter wave. The interference pattern does not attenuate because the momentum is completely uncertain when we choose a pre-selected state as the superposition of the eigenstate of the position, and the particle can reach the screen immediately after passing through the double-slit. If we choose a superposition of a Gaussian distribution as the pre-selected state, we can demonstrate the experimental result as the dashed curve in Fig. 3.2. However, we consider the superposition of the eigenstate of the position for simplicity.

The transition amplitude can be expressed by

$$K(\alpha) := \langle\psi|u_p(\alpha)U(T)|\phi\rangle, \tag{3.16}$$
$$u_p(\alpha) := \exp[-i\alpha p], \tag{3.17}$$

where the unitary operator $u_p(\alpha)$ expresses the shift of the post-selection alongside the screen by α. To determine the path, we introduce an identity operator to divide the transition amplitude $K(\alpha)$,

$$\mathbb{I} = \int_0^\infty dx|x\rangle\langle x| + \int_{-\infty}^0 dx|x\rangle\langle x|. \tag{3.18}$$

Substituting the identity operator (3.18) to (3.16), then we split the transition amplitude into to two parts:

$$\begin{aligned} K(\alpha) &= \langle\psi|u_p(\alpha)U(T)|\phi\rangle \\ &= \frac{\langle\psi|u_p(\alpha)U(T)|-x_i\rangle}{\sqrt{2}} + \frac{\langle\psi|u_p(\alpha)U(T)|x_i\rangle}{\sqrt{2}}. \end{aligned} \tag{3.19}$$

By using new states $|\phi_\pm\rangle = |\pm x_i\rangle/\sqrt{2}$, we define transition amplitudes as

$$K_\pm(\alpha) := \langle\psi|u_p(\alpha)U(T)|\phi_\pm\rangle. \tag{3.20}$$

The interference is caused by these two paths between $K_+(\alpha)$ and $K_-(\alpha)$. In the double-slit experiment, the post-selected state is the eigenstate of the position $|x_f\rangle$. Because $u_p^\dagger(\alpha)$ is the translation operator $u_p^\dagger(\alpha)|x_f\rangle = |x_f - \alpha\rangle$, $u_p^\dagger(\alpha)$ moves the position x_f to $x_f - \alpha$. The momentum weak value p_w, p_w^+ and p_w^- are

$$p_w = \frac{\langle\psi|pU(T)|\phi\rangle}{\langle\psi|U(T)|\phi\rangle} = m\frac{x_f + ix_i\tan\left(\frac{m}{\hbar}\frac{x_f x_i}{T}\right)}{T}, \tag{3.21}$$

$$p_w^\pm = \frac{\langle\psi|pU(T)|\phi_\pm\rangle}{\langle\psi|U(T)|\phi_\pm\rangle} = m\frac{x_f \mp x_i}{T}. \tag{3.22}$$

Because the imaginary part of the momentum weak values $p_w^\pm$ are zero, the index of interference becomes

$$\begin{aligned} \mathcal{I} &= \mathrm{Im}\left[p_w - p_w^-\frac{|K_-(0)|^2}{|K(0)|^2} - p_w^+\frac{|K_+(0)|^2}{|K(0)|^2}\right] \\ &= \mathrm{Im}\left[p_w\right] = m\frac{x_i\tan\left(\frac{m}{\hbar}\frac{x_f x_i}{T}\right)}{T}, \end{aligned} \tag{3.23}$$

from which the variation of interference terms is represented by the imaginary part of the weak value p_w, i.e., the index of interference is expressed by the imaginary part of the weak value p_w. Apparently, the index $\mathcal{I}$ becomes small when the interference pattern is constructive. In contrast, the index $\mathcal{I}$ diverges when the interference pattern is destructive: see Fig. 3.3.

We briefly explain the real part of the weak value p_w. The momentum weak values p_w^+ and p_w^- are contribution from the classical path between two eigenstates of the point, and coincides with the classical motion (we show this later). The real part of the weak value p_w is equal to the average of these two weak values $p_w^\pm$, $\mathrm{Re}\, p_w = (p_w^+ + p_w^-)/2$. Thus, the momentum weak value $\mathrm{Re}\, p_w$ is equivalent to the average of the momentum for each classical path.

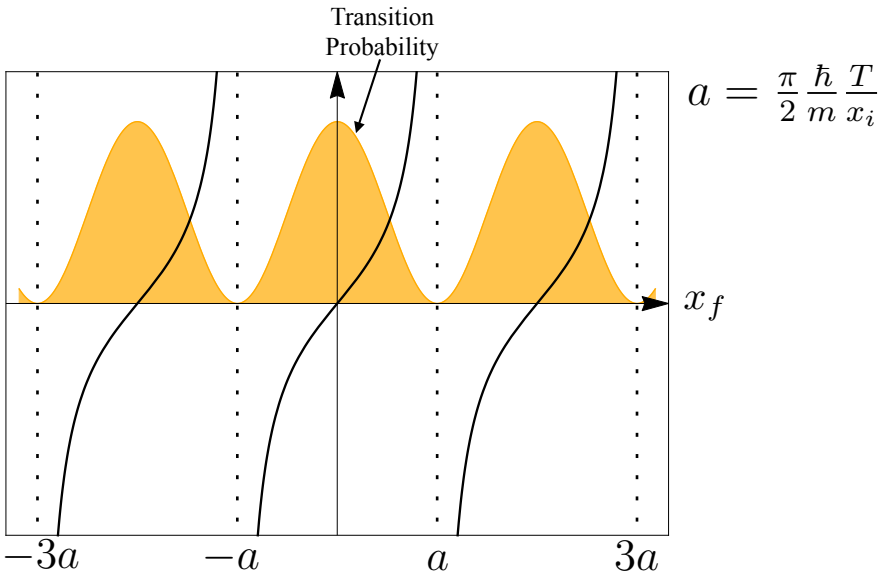

Figure 3.3: Orange filled curve is the transition probability. The thick line is the imaginary part of the momentum weak value (the index of interference). We have $a = \pi\hbar T/2mx_i$. Apparently the imaginary part is correspond to the interference pattern. The index diverges when the interference pattern is destructive. In contrast, the index becomes zero when the interference pattern is constructive.

3.2.1 A more general example for the double-slit experiment

Now, we prepare a more general pre-selection by exploiting a phase γ and a real number R,

$$|\varphi\rangle = \frac{1}{\sqrt{1+R^2}}\left(|x_i\rangle + R\mathrm{e}^{\mathrm{i}\gamma}|-x_i\rangle\right), \tag{3.24}$$

and the post-selection $|\psi\rangle = |x_f\rangle$. A non-trivial split for the transition amplitude can be realized by employing the following identity operator with phases θ and η,

$$\begin{aligned}\mathbb{I} \;=\; & \left(\mathrm{e}^{\mathrm{i}\eta}\cos\theta + \sin\theta\right)\left(\mathrm{e}^{-\mathrm{i}\eta}\cos\theta\int_0^\infty |x\rangle\langle x|dx + \sin\theta\int_{-\infty}^0 |x\rangle\langle x|dx\right) \\ & + \left(-\mathrm{e}^{\mathrm{i}\eta}\sin\theta + \cos\theta\right)\left(-\mathrm{e}^{-\mathrm{i}\eta}\sin\theta\int_0^\infty |x\rangle\langle x|dx + \cos\theta\int_{-\infty}^0 |x\rangle\langle x|dx\right),\end{aligned} \tag{3.25}$$

from which the transition amplitude is split into two parts,

$$\begin{aligned} K(\alpha) &:= \langle\psi|u_p(\alpha)U(T)|\varphi\rangle \\ &= K_{\varphi_+}(\alpha) + K_{\varphi_-}(\alpha), && (3.26)\\ K_{\varphi_\pm}(\alpha) &:= \langle\psi|u_p(\alpha)U(T)|\varphi_\pm\rangle, && (3.27)\\ |\varphi_+\rangle &:= \frac{\left(\mathrm{e}^{\mathrm{i}\eta}\cos\theta + \sin\theta\right)}{\sqrt{1+R^2}}\left(\mathrm{e}^{-\mathrm{i}\eta}\cos\theta|x_i\rangle + R\mathrm{e}^{\mathrm{i}\gamma}\sin\theta|-x_i\rangle\right), && (3.28)\\ |\varphi_-\rangle &:= \frac{\left(-\mathrm{e}^{\mathrm{i}\eta}\sin\theta + \cos\theta\right)}{\sqrt{1+R^2}}\left(-\mathrm{e}^{-\mathrm{i}\eta}\sin\theta|x_i\rangle + R\mathrm{e}^{\mathrm{i}\gamma}\cos\theta|-x_i\rangle\right), && (3.29)\end{aligned}$$

In this choice the index of interference becomes

$$\begin{aligned}
\mathcal{I} &= \mathrm{Im}\left[p_w - p_w^{\varphi_-}\frac{|K_{\varphi_-}(0)|^2}{|K(0)|^2} - p_w^{\varphi_+}\frac{|K_{\varphi_+}(0)|^2}{|K(0)|^2}\right] && (3.30)\\
&= m\frac{x_i}{T}\frac{2R\sin\left(2\frac{m}{\hbar}\frac{x_f x_i}{T}+\gamma\right)}{1+R^2+2R\cos\left(2\frac{m}{\hbar}\frac{x_f x_i}{T}+\gamma\right)}\\
&\quad -m\frac{x_i}{T}\frac{2R\sin^2(2\theta)\cos\eta\sin\left(\gamma+\frac{m}{\hbar}\frac{2x_f x_i}{T}+\eta\right)}{1+R^2+2R\cos\left(\gamma+\frac{m}{\hbar}\frac{2x_f x_i}{T}\right)}, && (3.31)\\
p_w &:= \frac{\langle\psi|pU(T)|\phi\rangle}{\langle\psi|U(T)|\phi\rangle}\\
&= m\frac{x_f}{T} - m\frac{x_i}{T}\frac{1-R^2}{1+R^2+2R\cos\left(2\frac{m}{\hbar}\frac{x_f x_i}{T}+\gamma\right)}\\
&\quad +\mathrm{i}m\frac{x_i}{T}\frac{2R\sin\left(2\frac{m}{\hbar}\frac{x_f x_i}{T}+\gamma\right)}{1+R^2+2R\cos\left(2\frac{m}{\hbar}\frac{x_f x_i}{T}+\gamma\right)}, && (3.32)\\
p_w^{\varphi_+} &:= \frac{\langle\psi|pU(T)|\varphi_+\rangle}{\langle\psi|U(T)|\varphi_+\rangle}\\
&= m\frac{x_f+x_i}{T} - 2m\frac{x_i}{T}\frac{\cos\theta}{\cos\theta+R\mathrm{e}^{\mathrm{i}\left(\frac{m}{\hbar}\frac{2x_f x_i}{T}+\gamma+\eta\right)}\sin\theta}, && (3.33)\\
p_w^{\varphi_-} &:= \frac{\langle\psi|pU(T)|\varphi_-\rangle}{\langle\psi|U(T)|\varphi_-\rangle}\\
&= m\frac{x_f+x_i}{T} + 2m\frac{x_i}{T}\frac{\sin\theta}{-\sin\theta+R\mathrm{e}^{\mathrm{i}\left(\frac{m}{\hbar}\frac{2x_f x_i}{T}+\gamma+\eta\right)}\cos\theta}, && (3.34)\\
|K(0)|^2 &= \frac{m}{4\pi\hbar T}\frac{1}{1+R^2}\left(1+R^2+2\cos\left(\frac{m}{\hbar}\frac{2x_f x_i}{T}+\gamma\right)\right) && (3.35)\\
|K_{\varphi_\pm}(0)|^2 &= \frac{(1\pm\sin(2\theta)\cos\eta)\,(\pm(1-R^2)\cos(2\theta)+1+R^2)}{4\pi\hbar T(1+R^2)}\\
&\quad \pm R\frac{(1\pm\sin(2\theta)\cos\eta)\sin(2\theta)\cos\left(\gamma+\frac{2\frac{m}{\hbar}x_f x_i}{T}+\eta\right)}{2\pi\hbar T(1+R^2)}, && (3.36)
\end{aligned}$$

from which we conclude that the index $\mathcal{I}$ depends on the choice of division (the choice of the phases θ and η) for the simple double-slit (thought) experiment. In our definition of the index of interference, if we put the parameters $\theta = \pi/4$ and $\eta = 0$ (it means we do not split the transition amplitude), the interference is not observed. In contrast, if we have $\theta = 0$ (the selection of the path is similar to that in the previous section, (3.18)), the interference is observed. The index $\mathcal{I}$ is equal to the imaginary part of the momentum weak value, Im p_w.

Up to this point, we assumed superposition of two-position eigenstates as the pre-selected state. To argue a more realistic version of the double-slit experiment, we should consider finite width slit; this kind of discussions will be presented in section 3.3 and section 3.4.

3.3 Fraunhofer diffraction

In the above discussion, we assumed that the slits have infinitesimally small width, and it is not realistic. It is well known that interference pattern appears on the screen when a particle passes a slit of a finite width. We consider the case in which the particle passes through each slit of a finite width 2σ and is diffracted, then we detect the particle on the screen. The pre-selected state is given by

$$|\phi\rangle = \int_{-\sigma}^{\sigma} dx\, |x\rangle, \tag{3.37}$$

and the post-selected state is the position eigenstate,

$$|\psi\rangle = |x_f\rangle. \tag{3.38}$$

The particle evolves under the free Hamiltonian $H = p^2/2m$. Let us consider the unitary operator $u_p(\alpha) = \exp(-\mathrm{i}\alpha p)$. The transition amplitude is

$$K(\alpha) = \langle\psi|u_p(\alpha)U(T)|\phi\rangle \tag{3.39}$$

$$= \frac{\mathrm{i}}{2}\sqrt{\frac{m}{\hbar}}\left(\mathrm{Erfi}\left[\frac{\left(\frac{1}{2}+\frac{\mathrm{i}}{2}\right)(x_f-\alpha-\sigma)}{\sqrt{\frac{\hbar T}{m}}}\right] - \mathrm{Erfi}\left[\frac{\left(\frac{1}{2}+\frac{\mathrm{i}}{2}\right)(x_f-\alpha+\sigma)}{\sqrt{\frac{\hbar T}{m}}}\right]\right), \tag{3.40}$$

$$\mathrm{Erfi}[z] = \frac{\mathrm{Erf}[\mathrm{i}z]}{\mathrm{i}} = \frac{2}{\mathrm{i}\sqrt{\pi}}\int_0^{\mathrm{i}z} \mathrm{e}^{-t^2} dt, \tag{3.41}$$

where $\mathrm{Erfi}[z]$ is known as the error function. To define the interference, we specify the path by

$$\mathbb{I} = \int_{-\infty}^{\infty} dx\, |x\rangle\langle x|. \tag{3.42}$$

The amplitude for each path is expressed as

$$K_x(\alpha) = \langle x_f|u_p(\alpha)U(T)|x\rangle. \tag{3.43}$$

The index of interference $\mathcal{I}$ is described as

$$\mathcal{I} = \mathrm{Im}\left[p_w - \int_{-\sigma}^{\sigma} dx\, p_{cl}\frac{|K_x(0)|^2}{|K(0)|^2}\right] = \mathrm{Im}\left[p_w\right], \tag{3.44}$$

$$p_w := \frac{\langle\psi|pU(T)|\phi\rangle}{\langle\psi|U(T)|\phi\rangle}, \tag{3.45}$$

$$p_{cl} := m\frac{x_f - x}{T}. \tag{3.46}$$

The index $\mathcal{I}$ is non-zero, so that the interference pattern can be seen. This interference effect is known as the Fraunhofer diffraction. The index of the interference is expressed by the

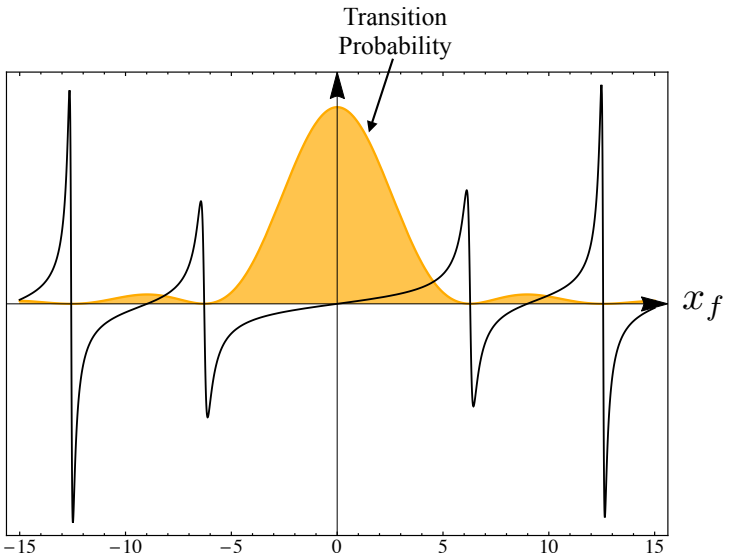

Figure 3.4: Orange filled curve is the transition probability. The thick line is the imaginary part of the momentum weak value (the index of interference). We have parameters $m = \hbar = T = 1$, $\sigma = 1/2$, and $-15 \leq x_f \leq 15$. Apparently the imaginary part corresponds to the interference pattern.

imaginary part of the momentum weak value. When the transition probability is extremal, the index $\mathcal{I}$ becomes zero: see Fig. 3.4.

Let us briefly note another trivial interpretation in which the index of interference becomes zero. Namely, we interpret that the transition probability is generated by the initial distribution of the particle in the width of 2σ, not by the interference, which coincides with the selection of only one path. Then, the index of interference $\mathcal{I}$ is equal to zero.

3.4 Double-slit of a finite width

In the above discussion, we assumed that the double-slit experiment with infinitesimally small width. Let us discuss the slit of a finite width. The center of the slits are at $\pm x_i$ and the width is given by 2σ, then the pre-selected state is expressed as

$$|\phi\rangle = \int_{x_i-\sigma}^{x_i+\sigma} dx\, |x\rangle + \int_{-x_i-\sigma}^{-x_i+\sigma} dx\, |x\rangle. \tag{3.47}$$

The post selected state is $|\psi\rangle = |x_f\rangle$ as before. We assume that interference is occurred when the particles from each slits are interfered, so that we put this condition by substituting the identity

$$\mathbb{I} = \int_{-\infty}^{0} dx\, |x\rangle\langle x| + \int_{0}^{\infty} dx\, |x\rangle\langle x|. \tag{3.48}$$

We define the states by

$$|\phi_\pm\rangle = \int_{\pm x_i-\sigma}^{\pm x_i+\sigma} dx\,|x\rangle. \tag{3.49}$$

The transition amplitudes can be written as

$$K(\alpha) = K_+(\alpha) + K_-(\alpha), \tag{3.50}$$

where

$$\begin{aligned} K_\pm(\alpha) &= \langle\psi|u_p(\alpha)U(T)|\phi_\pm\rangle & (3.51)\\ &= \frac{\mathrm{i}}{2}\sqrt{\frac{m}{\hbar}}\left(\mathrm{Erfi}\left[\frac{\left(\frac{1}{2}+\frac{\mathrm{i}}{2}\right)(x_f-\alpha\mp x_i-\sigma)}{\sqrt{\frac{\hbar T}{m}}}\right]+\mathrm{Erfi}\left[\frac{\left(\frac{1}{2}+\frac{\mathrm{i}}{2}\right)(x_f-\alpha\mp x_i+\sigma)}{\sqrt{\frac{\hbar T}{m}}}\right]\right). & (3.52)\end{aligned}$$

The index for interference is

$$\mathcal{I} = \mathrm{Im}\left[p_w - p_w^+\frac{|K_+(0)|^2}{|K(0)|^2} - p_w^-\frac{|K_-(0)|^2}{|K(0)|^2}\right], \tag{3.53}$$

$$p_w := \frac{\langle\psi|pU(T)|\phi\rangle}{\langle\psi|U(T)|\phi\rangle}, \tag{3.54}$$

$$p_w^\pm := \frac{\langle\psi|pU(T)|\phi_\pm\rangle}{\langle\psi|U(T)|\phi_\pm\rangle}. \tag{3.55}$$

In this case, the contribution from Fraunhofer interference is removed: see Fig. 3.5.

One may choose another case in which interference is caused by following path: each transition amplitudes can be written

$$K_x(\alpha) = \langle\psi|u_p(\alpha)U(T)|x\rangle, \tag{3.56}$$

then the index for interference is

$$\begin{aligned}\mathcal{I} &= \mathrm{Im}\left[p_w - \int_{-x_i-\sigma}^{-x_i+\sigma} dx\,p_{cl}\frac{|K_x(0)|^2}{|K(0)|^2} - \int_{x_i-\sigma}^{x_i+\sigma} dx\,p_{cl}\frac{|K_x(0)|^2}{|K(0)|^2}\right]\\ &= \mathrm{Im}\left[p_w\right], & (3.57)\end{aligned}$$

All effects including the Fraunhofer effect are taken into account.

Since the contribution from the Fraunhofer effect is small compared to the double-slit, we only can see a tiny difference between (3.53) and (3.57): see Fig. 3.5.

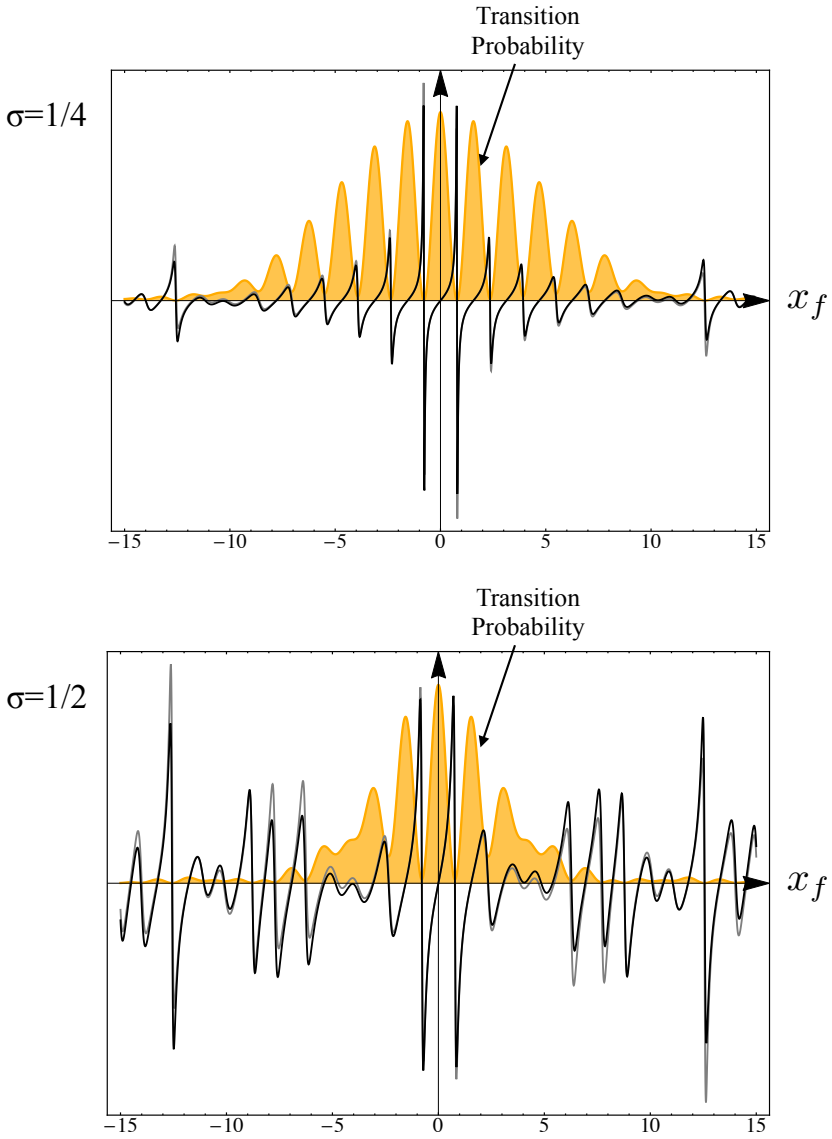

Figure 3.5: Orange filled curve is the transition probability. The thick and thin lines are the imaginary part of the momentum weak value (the index of interference). Apparently the imaginary part corresponds to the interference pattern. Thick and thin lines are describing (3.53) and (3.57), respectively. We have the parameters as $x_i = 2$, $-15 \leq x_f \leq 15$, and $m = \hbar = T = 1$ while $\sigma = 1/4$ and $\sigma = 1/2$.

3.5 Spin-1/2 system

In this section, by using the spin-1/2 system, we show a correlation between the spin weak value and interference. In the double-slit experiment, the classical path is obvious and selected without any doubt, but for the spin-1/2 system, we cannot decide the path a priori. A different choice of the path deduces a different interference effect.

The eigenstate for the Pauli matrix σ_z is written as $|+\rangle, |-\rangle$. As the pre- and post-selected states at $t = 0$ and $t = T$, we have

$$|\phi\rangle = |+\rangle, \tag{3.58}$$
$$|\psi\rangle = \exp[\mathrm{i}\theta\sigma_y]|+\rangle = \cos\theta|+\rangle + \sin\theta|-\rangle. \tag{3.59}$$

Here we consider the unitary transformation $u^\dagger_{\sigma_y}(\alpha) = \exp[\mathrm{i}\alpha\sigma_y]$ acting on the post-selection $|\psi\rangle$,

$$u^\dagger_{\sigma_y}(\alpha)|\psi\rangle = \exp[\mathrm{i}\alpha\sigma_y]|\psi\rangle = \cos(\theta+\alpha)|+\rangle + \sin(\theta+\alpha)|-\rangle, \tag{3.60}$$

and we assume that the state does not evolve in time: the unitary evolution is the identity operator $U(t) = \mathbb{I}$ for simplicity. The transition amplitude $K(\alpha)$ is defined as

$$K(\alpha) = \langle\psi|u_{\sigma_y}(\alpha)U(T)|\phi\rangle = \cos(\theta+\alpha), \tag{3.61}$$

and the transition probability is

$$P(\alpha) = |K(\alpha)|^2 = \cos^2(\theta+\alpha). \tag{3.62}$$

By taking the logarithmic derivative of the transition probability with respective to α, we obtain

$$\begin{aligned}\lim_{\alpha\to 0}\frac{1}{2}\frac{d}{d\alpha}\ln P(\alpha) &= \mathrm{Re}\left[\frac{\langle\psi| - \mathrm{i}\sigma_y U(T)|\phi\rangle}{\langle\psi|U(T)|\phi\rangle}\right] \\ &= \mathrm{Im}[\sigma_{yw}] = -\tan\theta.\end{aligned} \tag{3.63}$$

Let us set the two paths between the pre- and post-selected state. To do so, we define the eigenstate of the Pauli matrix σ_y by,

$$|R\rangle = \frac{1}{\sqrt{2}}(|+\rangle + \mathrm{i}|-\rangle), \tag{3.64}$$
$$|L\rangle = \frac{1}{\sqrt{2}}(|+\rangle - \mathrm{i}|-\rangle). \tag{3.65}$$

In this basis, the completeness relation is written as

$$\mathbb{I} = |R\rangle\langle R| + |L\rangle\langle L|, \tag{3.66}$$

and substituting (3.66) to (3.61),

$$\begin{aligned} K(\alpha) &= \langle\psi|u_{\sigma_y}(\alpha)|R\rangle\langle R|U(T)|\phi\rangle + \langle\psi|u_{\sigma_y}(\alpha)|L\rangle\langle L|U(T)|\phi\rangle \\ &= K_R(\alpha) + K_L(\alpha), \end{aligned} \tag{3.67}$$

$$K_L(\alpha) = \langle\psi|u_{\sigma_y}(\alpha)|L\rangle\langle L|U(T)|\phi\rangle = \frac{1}{2}\mathrm{e}^{-\mathrm{i}\alpha}, \tag{3.68}$$

$$K_R(\alpha) = \langle\psi|u_{\sigma_y}(\alpha)|R\rangle\langle R|U(T)|\phi\rangle = \frac{1}{2}\mathrm{e}^{\mathrm{i}\alpha}. \tag{3.69}$$

By defining these two path $K_L(\alpha), K_R(\alpha)$, we can argue the interference and see the cross term when we observe the transition probability,

$$\begin{aligned} P(\alpha) &= |K_R(\alpha) + K_L(\alpha)|^2 = |K_R(\alpha)|^2 + |K_L(\alpha)|^2 + 2\mathrm{Re}[K_R(\alpha)K_L^*(\alpha)] \\ &= \frac{1}{2} + \frac{1}{2}\cos(2\alpha). \end{aligned} \tag{3.70}$$

By substituting (3.11), the index of the interference is

$$\mathcal{I} = -\tan\theta. \tag{3.71}$$

We can take any basis, and if we change the basis in (3.66) as

$$\mathbb{I} = |+\rangle\langle+| + |-\rangle\langle-|, \tag{3.72}$$

the index of interference becomes $\mathcal{I} = 0$ which means there are no interference.

3.6 Summary

Interference of the particle is one of the most important aspects of quantum mechanics. To obtain physical interpretation of the weak value, we have utilized quantum interference. In the discussion of interference, we should specify what are interfering, which corresponds to the selection of the path. To do so, we must define the interference effect by subtracting the contribution of each path from the total transition probability. As we have seen in several examples, the interference effect very much depends on the choice of the path. By employing this definition, we have shown that the interference effect can be expressed in terms of the imaginary part of the weak value. In the double-slit experiment, the index of interference can be written by the momentum weak value. In the spin-1/2 system, the index of interference is represented by the spin weak value. We hope that our result of the relation between interference and the weak value will be helpful to understand the weak value more deeply in future.

Chapter 4

Weak trajectory

In quantum mechanics, it is well known that defining a trajectory is difficult because an observation of the position for the particle disturbs the momentum after the measurement (the uncertainty principle). This principle prevents us understanding the quantum mechanics intuitively. In this chapter, nevertheless, we regard the position weak value as the trajectory (which we call the weak trajectory) because the position weak value coincides with the classical trajectory in several examples. The correspondence between the position weak value and the classical trajectory was proposed by Tanaka in the semiclassical approximation [37]. As Tanaka pointed out, this property does not hold for general cases. We show that the position weak value can be interpreted as the average of the classical trajectory if one admits the complex probability [36, 38] while its imaginary part is relevant to interference [30]. We examine the condition in which the imaginary part of the position weak value vanish. Besides, by employing quantum eraser, we show that the weak value can specify which path the particle takes for an ensemble while the interference pattern remains. Since the weak value is defined for an ensemble, we cannot tell which path the particle takes for individual event. Thus, this weak value is consistent with the complementarity. And finally, the position weak value of the particle moving under the perfectly reflecting wall potential is examined.

4.1 Semiclassical approximation

We consider the quantum trajectory by employing the time-dependent position weak value. Prior to our work, the weak trajectory was examined by the position weak value in semiclassical approximation [37]. Semiclassical approximation shows us a direct correspondence of quantum mechanics to the classical mechanics. As he claimed in his paper, because semiclassical approximation is exact in several examples, it is important to investigate the trajectory based on the weak value. In this section, we review the previous work done by Tanaka [37].

Let us consider the following generating function for convenience,

$$Z(\xi(\cdot), A) \equiv \langle\psi|\underleftarrow{\exp}\left(-\frac{\mathrm{i}}{\hbar}\int_0^T (H - A\xi(t))dt\right)|\phi\rangle, \tag{4.1}$$

where $\underleftarrow{\exp}(\cdot)$ is the time ordered exponential. It is easily shown that the weak value can be derived by using the generating function,

$$\begin{aligned} A_w(t) &= \frac{\langle\psi|U(T-t)AU(t)|\phi\rangle}{\langle\psi|U(T)|\phi\rangle} \\ &= -\mathrm{i}\hbar\frac{\delta \ln Z(\xi(\cdot),A)}{\delta\xi(t)}\bigg|_{\xi(\cdot)=0}. \end{aligned} \tag{4.2}$$

From the stationary phase method, the generating function $Z(\xi(\cdot),A)$ can be exploited in the semiclassical approximation. Note that we ignore operator ordering which induces the result of only order $\mathcal{O}(\hbar)$, so it does not affect the following semiclassical argument. To implement the semiclassical approximation, an important assumption is asserted:

> *for infinitesimally small values of $\xi(\cdot)$, quantum interference between multiple classical trajectories do not present in the semiclassical evaluation* [37].

Namely, the classical trajectory (determined by the classical Hamiltonian $H(x,p)-A(x,p)\xi(t)$ with certain boundary conditions) is unique, and the semiclassical generating function follows this trajectory. The generating function $Z(\xi(\cdot),A)$ is supposed to be in a single form,

$$Z(\xi(\cdot),A) \sim E\,\exp(\mathrm{i}S/\hbar), \tag{4.3}$$

where E and S are the amplitude factor and classical action, respectively,

$$E \equiv \frac{1}{\sqrt{2\pi\hbar\partial x_f/\partial p(T)}}, \tag{4.4}$$

$$S \equiv \int_0^T (p(t)\dot{x}(t) - H + A\xi(t))\,dt. \tag{4.5}$$

The single term condition holds when $\hbar$ is small enough or the time scale is short. From the single term condition, the weak value is obtained

$$\begin{aligned} A_w &= \frac{\delta S}{\delta\xi(t)}\bigg|_{\xi(\cdot)\equiv 0} + \mathcal{O}(\hbar) \\ &= A(x(t),p(t)), \end{aligned} \tag{4.6}$$

where the value $A(x(t),p(t))$ is determined by the classical trajectory $x(t)$ and $p(t)$. One may change the boundary condition as long as the single term condition holds. In several examples, e.g. a coherent state, an anomalous (complex-valued) weak value can be obtained [37].

The complex valued trajectory has a significant role in the quantum phenomena such as tunneling effect though the complex valued trajectory is thought to be only a theoretical frame work. Tanaka mentioned that this complex valued trajectory may be observed based on the weak value. This result, however, relies on the semiclassical approximation. In the following sections, we examine the position weak value from its definition without employing any approximation.

4.2 Preliminary

Before discussing the main theme, let us consider a time-dependent weak value during $t \in [0, T]$. We denote the pre- and post-selected states as $|\phi\rangle$ and $|\psi\rangle$, respectively. Assuming the Hamiltonian $H = p^2/2m + V(x)$, the weak value of the observable A at time t is defined as

$$A_w(t) = \frac{\langle\psi|U(T-t)AU(t)|\phi\rangle}{\langle\psi|U(T)|\phi\rangle}, \tag{4.7}$$

where $U(t) = \exp(-\mathrm{i}Ht/\hbar)$. The useful relation can be derived by taking derivative with respect to time t,

$$\frac{dA_w(t)}{dt} = -\mathrm{i}\frac{1}{\hbar}\frac{\langle\psi|U(T-t)[A,H]U(t)|\phi\rangle}{\langle\psi|U(T)|\phi\rangle}. \tag{4.8}$$

Eq. (4.8) can be seen as a generalization of Ehrenfest theorem because Ehrenfest theorem is obtained when the post-selection is made by $|\psi\rangle = U(T)|\phi\rangle$.

We have useful relationships between the momentum and the position weak values from (4.8):

$$\dot{p}_w(t) = 0, \tag{4.9}$$

$$\dot{x}_w(t) = \frac{p_w(t)}{m}, \tag{4.10}$$

from which we conclude that $x_w(t)$ is real when x_w is real at two boundaries. In particular, if we have the position eigenstates for the pre-and post-selected states, the weak value $x_w(t)$ is real and coincides with the classical trajectory:

$$x_w(t) = \frac{\langle x_f|U(T-t)xU(t)|x_i\rangle}{\langle x_f|U(T)|x_i\rangle} = \frac{(x_f - x_i)t + x_iT}{T} = x_{cl}(t). \tag{4.11}$$

This classical picture seems to allow us to define the trajectory by the position weak value. We then define the weak trajectory by the position weak value. From (4.9) and (4.10), we may conclude that the weak value obeys the classical equation of motion. The classical picture can also be derived in the case in which the potential is quadratic in x and a moving particle under a constant magnetic field.

4.2.1 Harmonic oscillator

In this subsection, we show that, in a certain boundary condition, the position weak value coincides with the classical trajectory for the harmonic oscillator Hamiltonian. The harmonic oscillator Hamiltonian is given by

$$H = \frac{p^2}{2m} + \frac{m}{2}\omega^2 x^2, \tag{4.12}$$

where m and ω are a mass of the particle and the angular frequency, respectively. From (4.8), we obtain

$$\dot{p}_w(t) = -m\omega^2 x_w(t), \tag{4.13}$$
$$\dot{x}_w(t) = \frac{p_w(t)}{m}, \tag{4.14}$$

from which the weak values $x_w(t), p_w(t)$ are

$$x_w(t) = A\sin(\omega t) + B\cos(\omega t), \tag{4.15}$$
$$p_w(t) = m\omega A\cos(\omega t) - m\omega B\sin(\omega t), \tag{4.16}$$

where A and B are complex values. If the weak values are real at each boundary, A and B are real. In particular, if each boundary condition is described as the eigenstate of the position, these weak values coincide with the classical trajectories.

4.2.2 Constant magnetic field

Let us show the case in which a particle with an electric charge is moving under a constant magnetic field B. The Hamiltonian with an electromagnetic field is

$$H = \frac{(\mathbf{p} - e\mathbf{A})^2}{2m} + e\varphi, \tag{4.17}$$

where $\mathbf{A}$ and φ are a vector potential and a scalar potential, respectively. The electric charge is denoted by e. The magnetic field is parallel to the z-direction with strength B, and hence the vector potential and the scalar potential can be written as

$$\mathbf{A} = -\frac{B}{2}\hat{\mathbf{x}}y + \frac{B}{2}\hat{\mathbf{y}}x, \tag{4.18}$$
$$\varphi = 0, \tag{4.19}$$

where $\hat{}$ describes the unit vector. By substituting these values, we obtain the Hamiltonian

$$H = \frac{1}{2m}\left(\mathbf{p}^2 + eB(yp_x - xp_y) + \frac{e^2B^2}{4}x^2 + \frac{e^2B^2}{4}y^2\right), \tag{4.20}$$

where p_x, p_y represent the momentum in the x- and y-directions, respectively. We obtain the position and the momentum weak values with the Feynman Kernel for the Hamiltonian, but

instead of doing so we employ the useful relation (4.8). We show useful relationships bellow:

$$[x, p_x] = \mathrm{i}\hbar, \tag{4.21}$$
$$[x^2, p_x] = 2\mathrm{i}\hbar x, \tag{4.22}$$
$$[x, p_x^2] = 2\mathrm{i}\hbar p_x, \tag{4.23}$$
$$[x, H] = \mathrm{i}\hbar\frac{p_y}{m} + \mathrm{i}\hbar\frac{eBy}{2m}, \tag{4.24}$$
$$[y, H] = \mathrm{i}\hbar\frac{p_y}{m} - \mathrm{i}\hbar\frac{eBx}{2m}, \tag{4.25}$$
$$[p_x, H] = \mathrm{i}\hbar\frac{eBp_y}{2m} - \mathrm{i}\hbar\frac{e^2B^2}{4m}x, \tag{4.26}$$
$$[p_y, H] = -\mathrm{i}\hbar\frac{eBp_x}{2m} - \mathrm{i}\hbar\frac{e^2B^2}{4m}y. \tag{4.27}$$

By using these relationships, it turns out that the weak values satisfy

$$\dot{x}_w(t) = \frac{p_{x_w}(t)}{m} + \frac{eB}{2m}y_w(t), \tag{4.28}$$
$$\dot{y}_w(t) = \frac{p_{y_w}(t)}{m} - \frac{eB}{2m}x_w(t), \tag{4.29}$$
$$\dot{p}_{x_w}(t) = \frac{eB}{2m}p_{y_w}(t) - \frac{e^2B^2}{4m}x_w(t), \tag{4.30}$$
$$\dot{p}_{y_w}(t) = -\frac{eB}{2m}p_{x_w}(t) - \frac{e^2B^2}{4m}y_w(t). \tag{4.31}$$

These differential equations can be easily solved if we define the position and the momentum weak values by

$$z_w(t) := x_w(t) + \mathrm{i}y_w(t), \tag{4.32}$$
$$p_{z_w}(t) := p_{x_w}(t) + \mathrm{i}p_{y_w}(t). \tag{4.33}$$

The position and the momentum weak values, $z_w(t), p_{z_w}(t)$ satisfies the following differential equations:

$$\dot{z}_w(t) = \frac{p_{z_w}(t)}{m} - \mathrm{i}\frac{eB}{2m}z_w(t), \tag{4.34}$$
$$\dot{p}_{z_w}(t) = -\mathrm{i}\frac{B}{2m}p_{z_w}(t) - \frac{e^2B^2}{4m}z_w(t), \tag{4.35}$$

from which the position weak value $z_w(t)$ is

$$z_w(t) = A\cos\left(\frac{eB}{2m}t\right) + B\sin\left(\frac{eB}{2m}t\right), \tag{4.36}$$

where A and B are constant numbers which depend on the boundary conditions. Thus the weak values $x_w(t)$ and $y_w(t)$ are

$$x_w(t) = \mathrm{Re}\left[A\cos\left(\frac{eB}{2m}t\right) + B\sin\left(\frac{eB}{2m}t\right)\right], \tag{4.37}$$
$$y_w(t) = \mathrm{Im}\left[A\cos\left(\frac{eB}{2m}t\right) + B\sin\left(\frac{eB}{2m}t\right)\right]. \tag{4.38}$$

As the classical mechanics, if the particle is moving between two points, the trajectory is described by the circular motion in the $x-y$ plane.

In the next section, we examine an elementary, but an important example: the double-slit experiment. Feynman said the double-slit experiment cannot be explained by classical mechanics and is quintessential feature of quantum mechanics [2]. In the double-slit experiment, we show the weak value does not hold naive classical picture.

4.3 Double-slit experiment

As we have shown above, the weak value x_w between two points coincides with the classical trajectory. We consider the double-slit experiment as one of the simplest, but non-trivial examples: see Fig. 3.2. We are supposed to treat two-dimensional problem for the double-slit experiment. The weak value of position perpendicular to the screen, however, is also linear with respect to time t and if the pre-and post-selected states are eigenstates of position, the position weak value coincides with the classical trajectory as we have seen before. Hence, we ignore the position weak value perpendicular to the screen.

The pre-selected state is expressed by the superposition of two position eigenstates:

$$|\phi\rangle = \frac{1}{\sqrt{2}}\left(|x_i\rangle + |-x_i\rangle\right), \tag{4.39}$$

while the post-selected state is the position eigenstate $|x_f\rangle$. We assume the free Hamiltonian $H = p^2/2m$. The position weak value $x_w(t)$ can be obtained from (4.8). Instead of doing so, we employ the Feynman kernel (3.14) to derive the weak value. The position weak value $x_w(t)$ is

$$\begin{aligned}
x_w(t) &= \frac{\langle x_f|U(T-t)xU(t)|\phi\rangle}{\langle x_f|U(T)|\phi\rangle} \\
&= \frac{\langle x_f|U(T-t)xU(t)|x_i\rangle + \langle x_f|U(T-t)xU(t)|-x_i\rangle}{\langle x_f|U(T)|x_i\rangle + \langle x_f|U(T)|-x_i\rangle} \\
&= \frac{\langle x_f|U(T)|x_i\rangle x_w^+(t) + \langle x_f|U(T)|-x_i\rangle x_w^-(t)}{\langle x_f|U(T)|x_i\rangle + \langle x_f|U(T)|-x_i\rangle} \\
&= \frac{x_f t}{T} + \mathrm{i}\frac{x_i(t-T)\tan\left(\frac{m}{\hbar}\frac{x_f x_i}{T}\right)}{T}, \qquad (4.40) \\
x_w^{\pm}(t) &:= \frac{\langle x_f|U(T-t)xU(t)|\pm x_i\rangle}{\langle x_f|U(T)|\pm x_i\rangle} \\
&= \frac{(x_f \mp x_i)t \pm x_i T}{T}, \qquad (4.41)
\end{aligned}$$

from which we conclude that $x_w(t)$ is linear with respect to t: see Fig. 4.1. The position weak value $x_w^{\pm}(t)$ coincides with the classical motion of the massive particle. Observing the real part of the position weak value $x_w(t)$, it turns out that $x_w(t)$ is average value of the weak

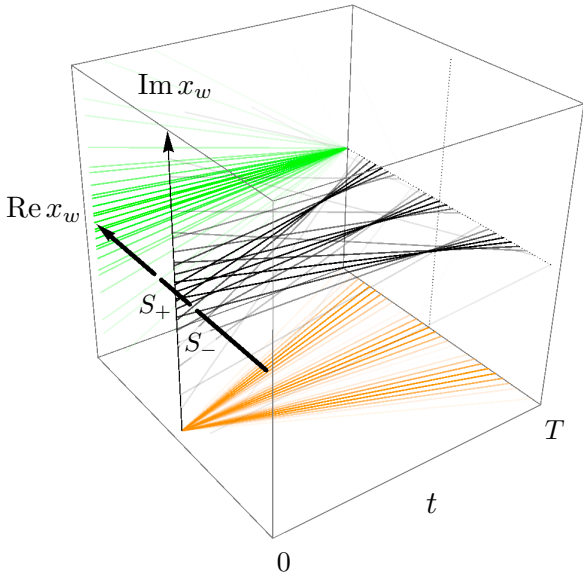

Figure 4.1: The position weak value $x_w(t)$ for various different post-selections with the density proportional to the transition probability $|\langle\psi|U(T)|\phi\rangle|^2$. The orange and green lines projected on the bottom and the left-back planes are drawn for the real and imaginary parts, respectively. The position weak value $x_w(t)$ is linear with respect to t.

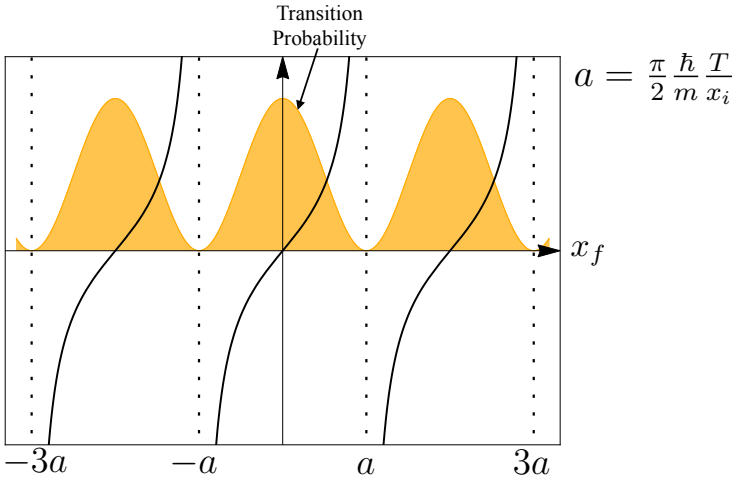

Figure 4.2: Black and gray lines are the real and imaginary parts of the weak value x_w at a certain time $t \in (0, T)$. We have $a = \pi\hbar T/2mx_i$. Orange filled curve is the transition probability. The imaginary part of the position weak value x_w diverges when the transition probability vanish. Thus, we infer that the interference effect is related to $\mathrm{Im}\, x_w(t)$.

values $x_w^{\pm}$ (classical trajectories). From (4.40), we can say that the imaginary part of the weak value disappears when the interference pattern is constructive (see Fig. 4.2).

We have shown the connection between the imaginary part of the weak value p_w and interference in (3.23). By using (4.9) and (4.10), the index of interference $\mathcal{I}$ can be related to the position weak value,

$$\mathrm{Im}\,\dot{x}_w(t) = \frac{1}{m}\mathrm{Im}\,p_w = \frac{\mathcal{I}}{m}. \tag{4.42}$$

The imaginary part of the position weak value $x_w(t)$ disappears when the transition probability is extremal as shown in Fig. 4.2.

As we have seen, the real part of the position weak value $x_w(t)$ can be seen as the average of the classical trajectories. We may consider the real part of the position weak value as the particle nature while the wave nature appears in the imaginary part [29, 30]. We examine whether this nature stands for another example in the next section.

4.4 Triple-slit experiment

To see the properties of the position weak value, we increase the number of the slit. We suppose the triple-slit experiment in which each slit is placed equally spaced.

The triple-slit can be expressed by choosing the pre-selected state as

$$|\phi\rangle = \frac{1}{\sqrt{3}}\left(|x_i\rangle + |0\rangle + |-x_i\rangle\right), \tag{4.43}$$

where $|\pm x_i\rangle$ and $|0\rangle$ describe the position of the slits while the post-selected state is the position eigenstate $|x_f\rangle$ which represents the position on the screen. The particle is governed by the free Hamiltonian. The position weak value $x_w(t)$ is

$$\begin{aligned}
x_w(t) &= \frac{\langle x_f|U(T-t)xU(t)|\phi\rangle}{\langle x_f|U(T)|\phi\rangle} \\
&= \frac{\langle x_f|U(T-t)xU(t)(|x_i\rangle + |0\rangle + |-x_i\rangle)}{\langle x_f|U(T)|x_i\rangle + \langle x_f|U(T)|0\rangle + \langle x_f|U(T)|-x_i\rangle} \\
&= \frac{tx_f}{T} + \frac{1}{T}\frac{2(T-t)x_i \sin\left(\frac{m}{\hbar}\frac{x_f x_i}{T}\right)\sin\left(\frac{m}{\hbar}\frac{x_i^2}{2T}\right)}{3 + 2\cos\left(\frac{m}{\hbar}\frac{2x_f x_i}{T}\right) + 4\cos\left(\frac{m}{\hbar}\frac{x_f x_i}{T}\right)\cos\left(\frac{m}{\hbar}\frac{x_i^2}{2T}\right)} \\
&\quad -\mathrm{i}\frac{2\left(1-\frac{t}{T}\right)x_i\left(\cos\left(\frac{m}{\hbar}\frac{x_f x_i}{T}\right) + \cos\left(\frac{m}{\hbar}\frac{x_i^2}{2T}\right)\right)\sin\left(\frac{m}{\hbar}\frac{x_f x_i}{T}\right)}{3 + 2\cos\left(\frac{m}{\hbar}\frac{2x_f x_i}{T}\right) + 4\cos\left(\frac{m}{\hbar}\frac{x_f x_i}{T}\right)\cos\left(\frac{m}{\hbar}\frac{x_i^2}{2T}\right)}.
\end{aligned} \tag{4.44}$$

The real part of the weak value x_w does not coincide with the average of the classical trajectories $\frac{x_f}{T}t$: there exists an extra term. The position weak value is linear with respect to the time t (see Fig. 4.3). The imaginary part of the weak value x_w vanishes when the derivative

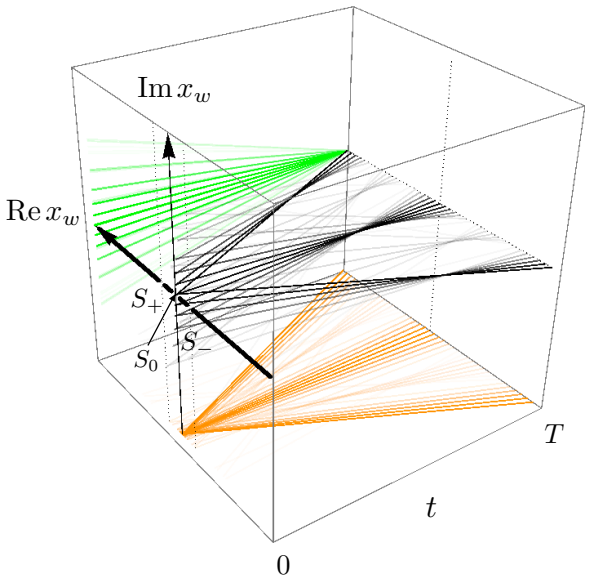

Figure 4.3: The position weak value $x_w(t)$ for various different post-selections with transparency proportional to the transition probability $|\langle\psi|U(T)|\phi\rangle|^2$. The orange and green lines projected on the bottom and the left-back planes are drawn for the real and imaginary parts, respectively.

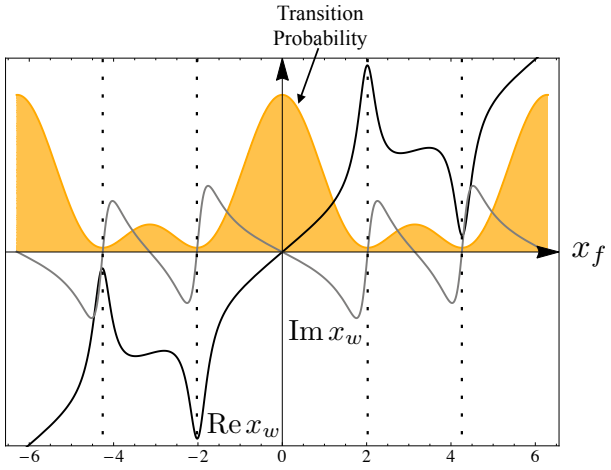

Figure 4.4: Black and gray lines are the real and imaginary parts of the weak value x_w at a certain time $t \in (0, T)$. We have parameters $m = \hbar = T = x_i = 1$ and $-6.3 \leq x_f \leq 6.3$. Orange filled curve is the transition probability. The imaginary part of the position weak value x_w vanishes when the transition probability becomes extremal. As the double-slit experiment, we infer that the interference effect is related to $\mathrm{Im}\, x_w(t)$.

of the transition probability with respect to x_f becomes zero. We can show the connection between the weak value and the interference same as (4.42): see Fig. 4.4.

The transition probability is proportional to

$$|\langle x_f|U(T)|\phi\rangle|^2 \propto 3 + 2\cos\left(\frac{m}{\hbar}\frac{2x_f x_i}{T}\right) + 4\cos\left(\frac{m}{\hbar}\frac{x_f x_i}{T}\right)\cos\left(\frac{m}{\hbar}\frac{x_i^2}{2T}\right),$$

and corresponds to the denominator of the position weak value. Thus, when the transition probability becomes small, the weak value increases unless the numerator also becomes small.

It has turned out that the real weak value for the triple-slit experiment cannot be written in the form of the average of the classical path, but if we admit the complex probability [36, 38], we obtain the picture that the position weak value is the average of the classical path [30] as we show that in the following section.

4.5 Multiple-slit experiment

In the above discussion, we have shown non-trivial example, and it turned out that the weak value is linear with respect to t. In this section, we elucidate this result to the multiple slit placed at $x_1, x_2, \ldots, x_n$, and show that the condition in which the weak value $x_w(t)$ is real. Besides, we show the real part of the position weak value is the average of the classical path if one admits the complex probability [36, 38].

The particles are localized at $x_1, x_2, \ldots, x_n$, and the corresponding state (pre-selected state) is

$$|\phi\rangle = \sum_{i=1}^{N} c_i|x_i\rangle, \quad c_i \in \mathbb{C}, \tag{4.45}$$

while the post-selected state remains to be the position eigenstate $|x_f\rangle$. The position weak value $x_w(t)$ is defined as

$$x_w(t) = \frac{\langle x_f|U(T-t)xU(t)|\phi\rangle}{\langle x_f|U(T)|\phi\rangle}, \tag{4.46}$$

and becomes,

$$\begin{aligned}
x_w(t) &= \frac{\sum_{i=1}^{N} c_i\langle x_f|U(T)|x_i\rangle x_{cl}^i(t)}{\sum_{i=1}^{N} c_i\langle x_f|U(T)|x_i\rangle} && (4.47)\\
&= \frac{t}{T}x_f + \frac{T-t}{T}\frac{\sum_{i=1}^{N} c_i\langle x_f|U(T)|x_i\rangle x_i}{\sum_{i=1}^{N} c_i\langle x_f|U(T)|x_i\rangle} && (4.48)\\
&= x_f + \frac{T-t}{T}\frac{\sum_{i=1}^{N} c_i\langle x_f|U(T)|x_i\rangle (x_i - x_f)}{\sum_{i=1}^{N} c_i\langle x_f|U(T)|x_i\rangle}, && (4.49)\\
x_{cl}^i(t) &= \frac{\langle x_f|U(T-t)xU(t)|x_i\rangle}{\langle x_f|U(T)|x_i\rangle} = \frac{t}{T}x_f + \frac{T-t}{T}x_i. && (4.50)
\end{aligned}$$

It is clear that (4.48) is linear with respect to t. Although the final position of this particle is at x_f, the initial value of $x_w(t)$ is a complex number and depends on x_i, x_f, and the coefficient c_i.

As discussed in [27], a real part of a weak value A is the conditional average of A and does not contain the effect of disturbance of a weak measurement though a imaginary part of weak value represents the disturbance. Besides this interpretation, we want to propose that (4.47) may be interpreted as an average of the classical trajectories weighted with the complex probability [36, 38]. To show that the weak value can be regarded as the average, we define the weight w_i as

$$w_i = \frac{c_i \langle x_f | U(T) | x_i \rangle}{\sum_i c_i \langle x_f | U(T) | x_i \rangle}, \tag{4.51}$$

and substitute w_i to (4.47),

$$x_w(t) \;=\; \sum_{i=1}^{N} w_i x_{cl}^i(t). \tag{4.52}$$

In general, the weight w_i has complex value and satisfies $\sum_i w_i = 1$. Thus, (4.52) may be regarded as the average of the classical path $x_{cl}^i(t)$ weighted with the complex probability w_i [30].

Let us consider the condition under which the imaginary part of the weak value vanishes,

$$\begin{aligned} x_w(t) &= \sum_{i=1}^{N} w_i x_{cl}^i(t) \\ &= \sum_{i=1}^{N} \frac{w_i + w_i^*}{2} x_{cl}^i(t) + \sum_{i=1}^{N} \frac{w_i - w_i^*}{2} x_{cl}^i(t), \end{aligned} \tag{4.53}$$

then the condition under which the imaginary part of the weak value $x_w(t)$ vanishes, $\mathrm{Im}[x_w(t)] = 0$, is equivalent to

$$\sum_{i=1}^{N} (w_i - w_i^*) x_{cl}^i(t) = 0. \tag{4.54}$$

Using (4.50), the condition (4.54) can be expressed as

$$\sum_{i=1}^{N} (w_i - w_i^*) x_i = 0. \tag{4.55}$$

Eq. (4.55) can be expressed in a more useful form [30]:

$$\frac{d}{dx_f} |\langle x_f | U(T) | \phi \rangle|^2 = 0. \tag{4.56}$$

We show the conditions (4.55) and (4.56) are equivalent. The condition (4.55) can be written as

$$
\begin{aligned}
(4.55) &= \sum_{i=1}^{N} \mathrm{Im} w_i x_i = \sum_{i=1}^{N} \mathrm{Im}\left[c_i \frac{\langle x_f|U(T)|x_i\rangle}{\langle x_f|U(T)|\phi\rangle} x_i\right] \\
&= \sum_{i=1}^{N} \mathrm{Im}\left[c_i \frac{\langle x_f|U(T)x|x_i\rangle}{\langle x_f|U(T)|\phi\rangle}\right] \\
&= \sum_{i=1}^{N} \mathrm{Im}\left[c_i \frac{\langle x_f|\left(x - \frac{p}{m}T\right)U(T)|x_i\rangle}{\langle x_f|U(T)|\phi\rangle}\right] \\
&= -\frac{T}{m}\sum_{i=1}^{N} \mathrm{Im}\left[c_i \frac{\langle x_f|pU(T)|x_i\rangle}{\langle x_f|U(T)|\phi\rangle}\right] \\
&= -\frac{T}{m}\mathrm{Im}\left[-\mathrm{i}\hbar\frac{\partial}{\partial x_f}\ln\langle x_f|U(T)|\phi\rangle\right] \\
&= \frac{\hbar T}{2m}\frac{\partial}{\partial x_f}\ln|\langle x_f|U(T)|\phi\rangle|^2. \qquad (4.57)
\end{aligned}
$$

So, the conditions (4.55) and (4.56) are the same.

We can rewrite the momentum and position weak values in terms of the logarithmic derivative with respect to x_f,

$$
\begin{aligned}
p_w(t) &= \frac{\langle x_f|U(T-t)pU(t)|\phi\rangle}{\langle x_f|U(T)|\phi\rangle} = \frac{\langle x_f|pU(T)|\phi\rangle}{\langle x_f|U(T)|\phi\rangle} \\
&= -\mathrm{i}\hbar\frac{d}{dx_f}\ln\langle x_f|U(T)|\phi\rangle, \qquad (4.58)
\end{aligned}
$$

from which the momentum weak value is independent of time t. Furthermore, the imaginary part of this weak value can be expressed as

$$
\mathrm{Im}\left[p_w(t)\right] = -\frac{\hbar}{2}\frac{d}{dx_f}\ln|\langle x_f|U(T)|\phi\rangle|^2, \qquad (4.59)
$$

from which (4.56) can be expressed by the momentum weak value. From (4.9), (4.10), and (4.58), we conclude that the weak value of the position is linear with respect to time t:

$$
x_w(t) = x_f - \mathrm{i}\hbar\frac{t-T}{m}\frac{d}{dx_f}\ln\langle x_f|U(T)|\phi\rangle. \qquad (4.60)
$$

The equivalence of (4.60) and (4.49) can be shown by using $\langle x_f|p = -\mathrm{i}\hbar d/dx_f\langle x_f|$.

Because (4.8) is independent on the pre- and post-selected states, we can show a more general condition under which the imaginary part of the weak value $x_w(t)$ vanishes. From (4.9) and (4.10), it turns out that the momentum weak value $p_w(t)$ is independent of time t. Thus, the position weak value $x_w(t)$ is purely real if $x_w(t)$ is a real number at each boundary.

So far, we have assumed $V(x) = 0$, but for a more general Hamiltonian $H = p^2/2m + V(x)$, we can derive more general relationships,

$$\dot{x}_w(t) = \frac{p_w(t)}{m}, \tag{4.61}$$

$$\dot{p}_w(t) = -\left\langle \frac{\partial V}{\partial x} \right\rangle_w (t), \tag{4.62}$$

$$\left\langle \frac{\partial V}{\partial x} \right\rangle_w (t) = \frac{\langle \psi | U(T-t) \frac{\partial V(x)}{\partial x} U(t) | \phi \rangle}{\langle \psi | U(T) | \phi \rangle}, \tag{4.63}$$

from which, if $x_w(t)$ is purely real at arbitrary time t, then $p_w(t)$ is also purely real. Taking contraposition of this, if $p_w(t)$ have an imaginary part, then $x_w(t)$ also must have an imaginary part.

Let us introduce another useful equation. Eq. (4.59) can be rewritten for the general potential as

$$\mathrm{Im}[p_w(T)] = -\frac{\hbar}{2} \frac{d}{dx_f} \ln |\langle x_f | U(T) | \phi \rangle|^2. \tag{4.64}$$

When one of the boundary conditions is the position eigenstate, (4.61) and(4.64) are useful to infer the weak value of the position for the general potential. In almost all of cases, we cannot say anything about the weak value except at its boundary because of the potential. The momentum weak value at the boundary can be calculated from (4.64), and if it has the imaginary part, then we can infer that the position weak value also has a complex value from (4.61).

4.6 The which-path information

So far, we could not observe the interference pattern and which path the particle took. To conquer this difficulty, introduce the spin-1/2 state to specify which path the particle takes. Depending on the choice at the screen, we can obtain the which-path information, or we can completely lose this information: the interference fringe reappears (Quantum eraser [7]). In this section, to get the which-path information, we introduce the spin-1/2 state to express the path of the particle and examine the trajectory of the particle in terms of the weak value [29, 38].

We assume that the particle is equipped with the spin-1/2 states, $|+\rangle$ and $|-\rangle$ (the eigenstates of the Pauli matrix σ_z). Initially, the particle is localized at $\pm x_i$ with a certain spin,

$$|\phi\rangle = \frac{1}{\sqrt{2}} (|x_i\rangle \otimes |+\rangle + |-x_i\rangle \otimes |-\rangle). \tag{4.65}$$

We obtain the path of the particle if we post-select the eigenstate of the Pauli matrix, $|+\rangle$ (or $|-\rangle$), on the screen. This measurement, however, destroys the interference pattern on the screen. This kind of discussion has been done by using a polarization of photon and is known

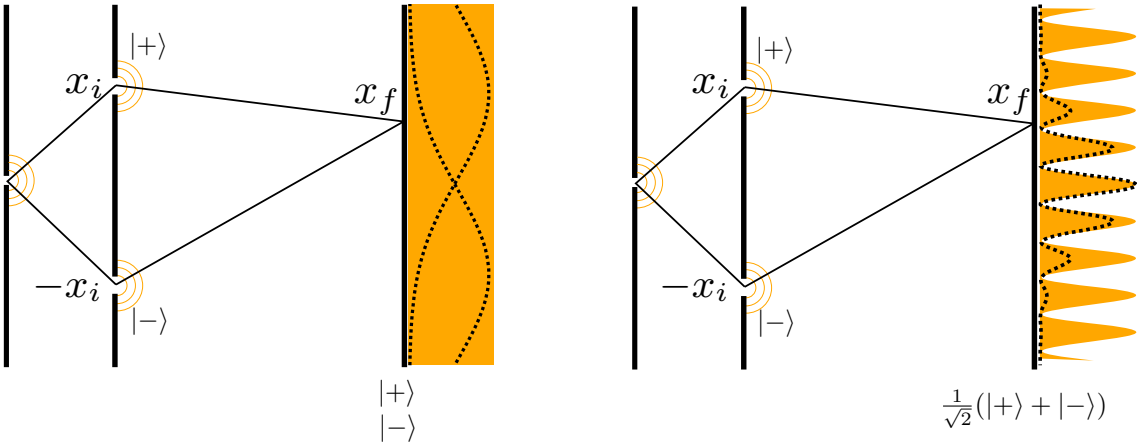

Figure 4.5: The double-slit thought experiment with the spin-1/2 state. The particle is localized around $S_\pm$ at time $t = 0$ with the spin state $|\pm\rangle$ and arrived at x_f at time $t = T$. When one observes which path the particle takes, the interference is washed away: the figure on the left. However, when the which-path information is completely lost by the post-selection, the interference pattern is reappeared: the figure on the right. The orange filled curve represents the superposition of the position eigenstate with the spin as the pre-selected state. If one prepare the superposition of the Gaussian state instead of the position eigenstate(and the spin state), the transition probability becomes more realistic and is drawn in the dashed curve.

as "quantum eraser" [7, 39, 40, 41]. We choose a post-selected state representing a point on the screen with a certain spin-1/2 state,

$$|\psi\rangle = |x_f\rangle \otimes [\cos(\theta/2)|+\rangle + \mathrm{e}^{\mathrm{i}\eta}\sin(\theta/2)|-\rangle], \tag{4.66}$$

where η is a real number that describes the phase. Depending on the choice of the post-selection, the interference pattern on the screen is changed. For $\theta = 0, \pi$, the interference pattern is washed away because which path the particle takes has been completely observed. Instead, by putting $\theta = \frac{\pi}{2}$, we recover the interference fringes, but we completely lose the which-path information (see Fig. 4.5). Let us define the spin-tagged position operator by

$$x^\pm = x \otimes |\pm\rangle\langle\pm|. \tag{4.67}$$

The position operator x is expressed by the sum of $x^\pm$,

$$x \otimes \mathbb{I} = x^+ + x^-. \tag{4.68}$$

We assume that the particle evolves under the free Hamiltonian $H = p^2/2m \otimes \mathbb{I}$ so that the spin state does not change during the unitary evolution $U(t)$. The spin-tagged position weak

values $x_w^{\pm}(t)$ are

$$
\begin{aligned}
x_w^{+}(t) &= \frac{\langle\psi|U(T-t)x^{+}U(t)|\phi\rangle}{\langle\psi|U(T)|\phi\rangle}, \\
&= \frac{(t(x_f-x_i)+Tx_i)\cos(\theta/2)}{T\left(\cos(\theta/2)+\mathrm{e}^{\mathrm{i}\chi}\sin(\theta/2)\right)} && (4.69) \\
&= \frac{\cos(\theta/2)}{\cos(\theta/2)+\mathrm{e}^{\mathrm{i}\chi}\sin(\theta/2)}x_{cl}^{+}(t), && (4.70) \\
x_w^{-}(t) &= \frac{\langle\psi|U(T-t)x^{-}U(t)|\phi\rangle}{\langle\psi|U(T)|\phi\rangle}, \\
&= \frac{(t(x_f+x_i-Tx_i))\sin(\theta/2)}{T\left(\sin(\theta/2)+\mathrm{e}^{-\mathrm{i}\chi}\cos(\theta/2)\right)}, && (4.71) \\
&= \frac{\sin(\theta/2)}{\sin(\theta/2)+\mathrm{e}^{-\mathrm{i}\chi}\cos(\theta/2)}x_{cl}^{-}(t), && (4.72)
\end{aligned}
$$

where χ is equals to $2mx_fx_i/\hbar T-\eta$, and $x_{cl}^{\pm}(t)$ is the classical trajectory defined in (4.41). It is easily shown that, if we put $\theta=\pi/2$, $\mathrm{Re}\,x_w^{\pm}$ is proportional to the classical trajectory, i.e., $\mathrm{Re}\,x_w^{\pm}=x_{cl}^{\pm}/2$. Roughly speaking, this discrepancy can be explained by the following picture: the spin-tagged position weak value is equal to the value of the classical trajectory times the probability of finding the particle with the spin $|\pm\rangle\langle\pm|$. The imaginary part of the weak value $x^{\pm}(t)$ can be still understood in terms of the interference: see Appendix B.

Since we have post-selected the particle at the position x_f, the particle must be at the position x_f. To adjust the disagreement between classical trajectories and $\mathrm{Re}\,x_w^{\pm}(t)$, we define re-scaled weak value $\tilde{x}_{\pm}^{w}(t)$ so that $\tilde{x}_{\pm}^{w}(T)$ is equal to x_f,

$$\tilde{x}_w^{\pm}(t)=x_{cl}^{\pm}(t). \tag{4.73}$$

In Fig. 4.6, the orange and the green lines denote the real part of $x_w^{+}(t)$ and $x_w^{-}(t)$, respectively, and the density of these lines are proportional to the transition probability. If we obtain the path of the particle, the interference fringes are washed away. However, by implementing the weak measurement, we can show the path of the particle without destroying the interference pattern. Besides, we can also show the real part of these weak values correspond to the classical trajectory. It seems paradoxical because we observe the trajectory of the particle and the interference pattern simultaneously. Measuring wavelike and particlelike behavior together contradicts the complementarity. To measure weak values, we have to prepare an ensemble of the initial state. The spin-tagged position weak value is the result of many trials, and for each trial the weak value does not tell us which path the particle takes. Thus, the complementarity is satisfied because we couldn't observe the which-path information for each event.

We can generalize this result by introducing the multiple-slit experiment and a set of N states $\{|i\rangle\}$ to specify which path the particle takes. We begin by preparing the pre-selected state as

$$|\phi\rangle=\sum_{i=1}^{N}c_i|x_i\rangle\otimes|i\rangle, \qquad c_i\in\mathbb{C}. \tag{4.74}$$

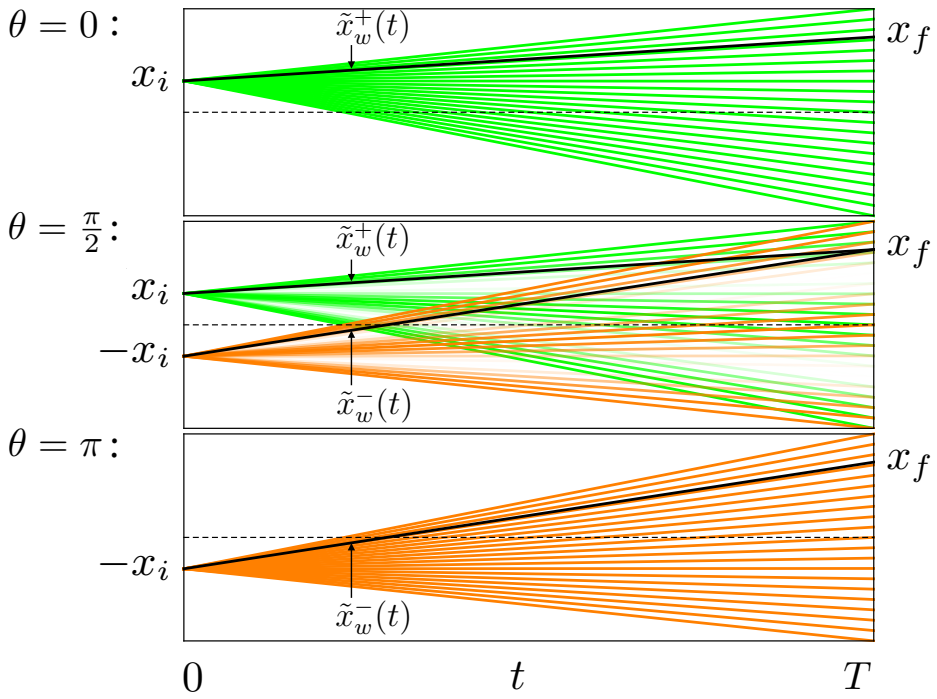

Figure 4.6: The position (with the spin) weak value $\tilde{x}_w^{\pm}(t)$ with various post-selection x_f while changing the parameter $\theta = 0, \pi/2, \pi$. The green and orange lines describe $\tilde{x}_w^+(t)$ and $\tilde{x}_w^-(t)$, respectively, and density is proportional to the transition probability $|\langle\psi|U(T)|\phi\rangle|^2$.

Usually, if one gets the which-path information, it will destroy the interference pattern, but we can recover interference instead of obtaining its path. This choice can be realized by the post-selection,

$$|\psi\rangle = \sum_{i=1}^{N} e_i |x_f\rangle \otimes |i\rangle, \qquad e_i \in \mathbb{C}. \tag{4.75}$$

As we can see (4.75), if we choose $e_i = \delta_{ij}$ for all i and some j, we observe the path, so that the interference pattern is washed away. In contrast, if $e_i = 1/\sqrt{N}$, we find the interference patten although we lose the which-path information. Intermediately, to observe the specific particle from one of the slits i, define the spin-tagged position operator x^i,

$$x^i = x \otimes |i\rangle\langle i|, \tag{4.76}$$

where $\sum_i x^i = x \otimes \mathbb{I}$. The spin-tagged position weak value $x_w^i(t)$ becomes

$$\begin{aligned} x_w^i(t) &= \frac{\langle\psi|U(T-t)x^iU(t)|\phi\rangle}{\langle\psi|U(T)|\phi\rangle} \\ &= \frac{x_{cl}^i(t)c_i e^* \langle x_f|U(T)|x_i\rangle}{\sum_i c_i \langle x_f|U(T)|x_i\rangle}, \end{aligned} \tag{4.77}$$

where $x_{cl}^i(t)$ is the classical trajectory defined in (4.50). To simplify the weak value, we define

weight w_i as

$$w_i = \frac{c_i e_i^* \langle x_f|U(T)|x_i\rangle}{\sum_i c_i e_i^* \langle x_f|U(T)|x_i\rangle}. \tag{4.78}$$

The weight w_i, in general, has a complex valued number and satisfies $\sum_{i=1}^{N} w_i = 1$ as complex probability [36, 38]. By using (4.78), we can rewrite the weak value $x_w^i(t)$,

$$x_w^i(t) = x_{cl}^i w_i. \tag{4.79}$$

This value is proportional to the classical value. To adjust this discrepancy, we define the re-scaled weak value

$$\tilde{x}_w^i(t) := \frac{x_w^i(t)}{w_i} = x_{cl}^i(t), \tag{4.80}$$

where we require the criteria that the weak trajectory corresponds to x_f at time $t = T$ (because we have already known the particle is at x_f by the post-selection). By specifying its final position, we can infer its initial position, and this re-scaled weak value corresponds to the classical trajectory.

4.7 Superposition of an infinite number of the position eigenstate

So far, we assumed a superposition of the discrete state for the pre-selection. In this section we consider the following state as the pre-selected state for the later discussion:

$$|\phi\rangle = \int dx_i c(x_i)|x_i\rangle, \quad c(x_i) \in \mathbb{C}, \tag{4.81}$$

which describes generalization of the multiple-slit experiment (4.45). As the post-selected state, we consider the position eigenstate $|x_f\rangle$. The particle evolves under the free Hamiltonian. In this case, the position weak value is

$$\begin{aligned} x_w(t) &= \frac{\langle x_f|U(T-t)xU(t)|\phi\rangle}{\langle x_f|U(T)|\phi\rangle} \\ &= \frac{\int dx_i c(x_i)\langle x_f|U(T-t)xU(t)|x_i\rangle}{\int dx_i c(x_i)\langle x_f|U(T)|x_i\rangle} \\ &= \frac{\int dx_i c(x_i)\langle x_f|U(T)|x_i\rangle x_{cl}^i(t)}{\int dx_i c(x_i)\langle x_f|U(T)|x_i\rangle}, \end{aligned} \tag{4.82}$$

where $x_{cl}^i(t)$ is the classical trajectory defined in (4.50). To simplify this expression, we introduce $w(x)$,

$$w(x) = \frac{c(x)\langle x_f|U(T)|x\rangle}{\int c(x)\langle x_f|U(T)|x\rangle}, \tag{4.83}$$

which, in general, is a complex number and satisfies $\int dx w(x) = 1$. If one admits the complex probability, the position weak value can be written by the form of the average of classical path [30],

$$x_w(t) = \int dx_i \, w(x_i) x^i_{cl}(t). \tag{4.84}$$

The condition in which the imaginary part of the weak value disappears can be expressed,

$$\int dx_i (w(x_i) - w^*(x_i)) x^i_{cl}(t) = 0, \tag{4.85}$$

from which we will see only the time independent term:

$$\int dx_i (w(x_i) - w^*(x_i)) x_i = 0. \tag{4.86}$$

Eq. (4.86) can be expressed exactly same as (4.56) though we omit the derivation.

For example, we put the pre- and post-selected states as the momentum eigenstate $|p\rangle$ and the position eigenstate $|x_f\rangle$, respectively. Then, one finds that the position weak value x_w becomes,

$$\begin{aligned} x_w(t) &= \frac{\langle x_f | U(T-t) x U(t) | p \rangle}{\langle x_f | U(T) | p \rangle} \\ &= \frac{\int \frac{dx_i}{\sqrt{2\pi\hbar}} \exp\left[\mathrm{i}\frac{p x_i}{\hbar}\right] \langle x_f | U(T-t) x U(t) | x_i \rangle}{\int \frac{dx_i}{\sqrt{2\pi\hbar}} \exp\left[\mathrm{i}\frac{p x_i}{\hbar}\right] \langle x_f | U(T) | x_i \rangle} \\ &= \frac{\int \frac{dx_i}{\sqrt{2\pi\hbar}} \exp\left[\mathrm{i}\frac{p x_i}{\hbar}\right] \langle x_f | U(T) | x_i \rangle x^i_w(t)}{\int \frac{dx_i}{\sqrt{2\pi\hbar}} \exp\left[\mathrm{i}\frac{p x_i}{\hbar}\right] \langle x_f | U(T) | x_i \rangle}. \end{aligned} \tag{4.87}$$

It is easily shown that the position weak value $x_w(t)$ is

$$x_w(t) = \frac{\langle x_f | U(T-t) x U(t) | p \rangle}{\langle x_f | U(T) | p \rangle} = x_f + \frac{p}{m}(t-T), \tag{4.88}$$

and similarly the momentum weak value $p_w(t)$ is

$$p_w(t) = \frac{\langle x_f | U(T-t) p U(t) | p \rangle}{\langle x_f | U(T) | p \rangle} = p, \tag{4.89}$$

We can realize (4.88) and (4.89) in a classical way: the particle has momentum p at $t = 0$ and, moving along side the x-direction until $t = T$, get at x_f. This can also be derived from (4.9) and (4.10). Since $|p\rangle$ is the momentum eigenstate, the momentum weak value is

$$p_w(t) = p. \tag{4.90}$$

At $t = T$, $x_w(t = T)$ correspond to its final position x_f. Hence we obtain

$$x_w(t) = x_f + \frac{p}{m}(t-T). \tag{4.91}$$

Obviously, the position weak value $x_w(t)$ is purely real, and it can be easily shown that the condition (4.56) is satisfied,

$$\frac{d}{dx_f}\left|\langle x_f|U(T)|p\rangle\right|^2 = \frac{d}{dx_f}\left|\mathrm{e}^{-\mathrm{i}\frac{p^2}{2m\hbar}T}\frac{\mathrm{e}^{\mathrm{i}\frac{x_f p}{\hbar}}}{\sqrt{2\pi\hbar}}\right|^2$$
$$= \frac{d}{dx_f}\frac{1}{2\pi\hbar} = 0.$$

We consider a more non-trivial example for the reality of the weak value. We have the pre-selected state as the complex Gaussian distribution,

$$|\phi\rangle = \int dx \mathrm{e}^{\mathrm{i}\alpha x^2+\mathrm{i}\beta x}|x\rangle, \tag{4.92}$$

where α and β are real numbers and do not depend on x_f. Note that this pre-selected state is neither eigenstate of the position nor the momentum. The transition amplitude $\langle x_f|U(T)|\phi\rangle$ is

$$\langle x_f|U(T)|\phi\rangle = \frac{\exp\left[\mathrm{i}\frac{2x_f^2\alpha+2x_f\beta-\frac{\hbar}{m}T\beta^2}{2+4\frac{\hbar}{m}T\alpha}\right]}{\sqrt{1+2\frac{\hbar}{m}T\alpha}}. \tag{4.93}$$

The weak values $p_w(t)$ and $x_w(t)$ are

$$p_w(t) = \hbar\frac{x_f\alpha+\frac{\beta}{2}}{\frac{\hbar}{m}T\alpha+\frac{1}{2}}, \tag{4.94}$$

$$x_w(t) = x_f - (T-t)\frac{\hbar}{m}\frac{x_f\alpha+\frac{\beta}{2}}{\frac{\hbar}{m}T\alpha+\frac{1}{2}}, \tag{4.95}$$

and these weak values are purely real. The conditions (4.86) and (4.56) is also consistent, and can be checked straightforwardly.

4.8 Lloyd's mirror

In this section, we consider the Hamiltonian with the potential. So far, we have discussed some simple cases including the Hamiltonian with the quadratic potential and the particle moving under a constant magnetic field can coincide the classical motion in several situations. However, in this section, we show non-trivial example which does not obey the classical trajectory even if one selects position eigenstates for the pre- and post selections [30].

Let us consider the potential $V(x)$ as $V(x) = \infty$ for $x < 0$ and $V(x) = 0$ for $x \geq 0$. The boundary condition is that the wave function vanishes at $x = 0$, which is known as Dirichlet boundary condition. More detailed discussion about the different boundary condition is in

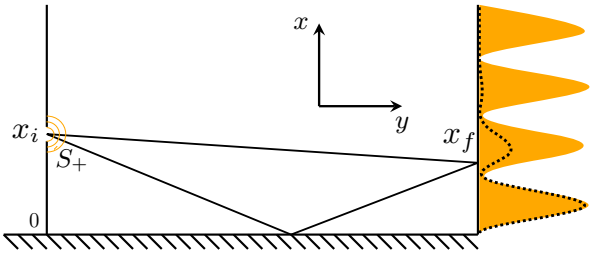

Figure 4.7: Lloyd's mirror experiment. The particle is localized around S_+ at time $t = 0$ and arrived at x_f at time $t = T$. In classical optics, the light can take the path toward the screen via the wall (mirror) and straight forwardly toward the screen. This particle cause interference on the screen, and the orange filled curve represents the interference fringes (the transition probability) especially when one choose the position eigenstate as the pre-selected state. If one prepares the Gaussian state instead of the position eigenstate, the transition probability becomes more realistic and is drawn in the dashed curve.

[42]. We assume that the particle moves under the free Hamiltonian in the y-direction, and reaches at the screen as Fig. 4.7. In general, we must consider two-dimensional system. However, as long as we focus on the weak value along the x-direction, we can ignore the contribution from the y-direction because of its definition. Hence, our main concern is one-dimensional system with the perfectly reflecting wall potential.

We obtain the Feynman kernel $K(x,t;x_0,t_0) = \langle x|U(t,t_0)|x_0\rangle$ by substituting a set of eigenstates of the Hamiltonian $\{|\chi_k\rangle\}$,

$$\begin{aligned} K(x,t;x_0,t_0) &= \langle x|U(t,t_0)|x_0\rangle \\ &= \int dk\, \langle x|U(t,t_0)|\chi_k\rangle\langle\chi_k|x_0\rangle \\ &= \int dk\, \langle x|\mathrm{e}^{-\mathrm{i}H(t-t_0)/\hbar}|\chi_k\rangle\langle\chi_k|x_0\rangle \\ &= \int dk\, \chi_k(x)\chi_k^*(x_0)\mathrm{e}^{-\mathrm{i}E_k(t-t_0)/\hbar}, \end{aligned} \tag{4.96}$$

where E_k is the eigenvalue of the Hamiltonian for the eigenstate $|\chi_k\rangle$. From the Dirichlet boundary condition, it is well known that the solution for the Schrödinger equation is superposition of the plane wave,

$$\chi_k(x) = \langle x|\chi_k\rangle = \frac{1}{\sqrt{2L}}\left(\mathrm{e}^{\mathrm{i}kx} - \mathrm{e}^{-\mathrm{i}kx}\right), \tag{4.97}$$

where L is $L=\pi$. By using (4.96), one can write the Feynman kernel,

$$\begin{aligned} K(x,t;x_0,t_0) &= \int dk \chi_k(x)\chi_k^*(x_0)\mathrm{e}^{-\mathrm{i}E_k(t-t_0)/\hbar} \\ &= \int dk \chi_k(x)\chi_k^*(x_0)\mathrm{e}^{-\mathrm{i}\frac{\hbar^2k^2}{2m}(t-t_0)\frac{1}{\hbar}} \\ &= \sqrt{\frac{m}{2\pi\mathrm{i}\hbar(t-t_0)}}\left(\mathrm{e}^{\mathrm{i}m\frac{(x-x_0)^2}{2\hbar(t-t_0)}}-\mathrm{e}^{\mathrm{i}m\frac{(x+x_0)^2}{2\hbar(t-t_0)}}\right). \end{aligned} \tag{4.98}$$

This is similar to the double-slit experiment except for the phase. The domain of this Feynman kernel is defined in $x \geq 0$. The transition probability $P(x,t;x_0,t_0)$ is

$$P(x,t;x_0,t_0)=|K(x,t;x_0,t_0)|^2=\frac{2m}{\pi\hbar(t-t_0)}\sin^2\left(m\frac{xx_0}{\hbar(t-t_0)}\right). \tag{4.99}$$

Naturally, the interference pattern can be seen and is known as Lloyd's mirror. One may expect that the position weak value is same as the double-slit experiment, but the behavior of the weak value is completely different. We will examine the weak value of the position. For simplicity, the pre- and post-selected states are position eigenvalues $|x_i\rangle$ and $|x_f\rangle$, respectively, and the position weak value $x_w(t)$ is defined,

$$x_w(t) = \frac{\langle x_f|U(T-t)xU(t)|x_i\rangle}{\langle x_f|U(T)|x_i\rangle}=\frac{\int_0^\infty dx K(x_f,T;x,T-t)xK(x,t;x_i,0)}{K(x_f,T;x_i,0)}. \tag{4.100}$$

This weak value can be rewritten by error function $\mathrm{Erfi}(z)$ and is not linear with respect to t anymore,

$$\begin{aligned} x_w(t) = &\ \mathrm{i}\frac{\mathrm{e}^{-\mathrm{i}\frac{m}{\hbar}\frac{x_fx_i}{T}}(t(x_f-x_i)+Tx_i)\mathrm{Erfi}\left[\left(\frac{1}{2}+\frac{\mathrm{i}}{2}\right)\frac{(t(x_f-x_i)+Tx_i)}{\sqrt{tT(T-t)}}\sqrt{\frac{m}{\hbar}}\right]}{\left(\mathrm{e}^{\mathrm{i}\frac{m}{\hbar}\frac{x_fx_i}{T}}-\mathrm{e}^{-\mathrm{i}\frac{m}{\hbar}\frac{x_fx_i}{T}}\right)T} \\ &+\mathrm{i}\frac{\mathrm{e}^{\mathrm{i}\frac{m}{\hbar}\frac{x_fx_i}{T}}(t(x_f+x_i)-Tx_i)\mathrm{Erfi}\left[\left(\frac{1}{2}+\frac{\mathrm{i}}{2}\right)\frac{(-t(x_f+x_i)+Tx_i)}{\sqrt{tT(T-t)}}\sqrt{\frac{m}{\hbar}}\right]}{\left(\mathrm{e}^{\mathrm{i}\frac{m}{\hbar}\frac{x_fx_i}{T}}-\mathrm{e}^{-\mathrm{i}\frac{m}{\hbar}\frac{x_fx_i}{T}}\right)T}. \end{aligned} \tag{4.101}$$

The weak value $x_w(t)$ can be calculated numerically, and we show the behavior of the weak value $x_w(t)$ in Fig. 4.8. Note that the real part of the position weak value $\mathrm{Re}\ x_w(t)$ behaves wildly when the interference patten destructive. By using (4.61), whether the weak value $x_w(t)$ has a complex number can be shown without calculate $x_w(t)$. $\mathrm{Im}\ p_w(T)$ is derived from the transition probability,

$$\mathrm{Im}\ p_w(T)=-\frac{1}{2}\frac{\partial}{\partial x_f}\ln|\langle x_f|U(T)|x_i\rangle|^2, \tag{4.102}$$

and is easily shown that $\mathrm{Im}\ p_w(T)=-mx_i\cot\left(mx_fx_i/\hbar T\right)/\hbar T$. Thus, in general, $p_w(T)$ is a complex number, so we can infer that $\mathrm{Im}\ x_w(T)$ also has a complex number from (4.61) even though $x_w(t)$ is a real number at boundaries.

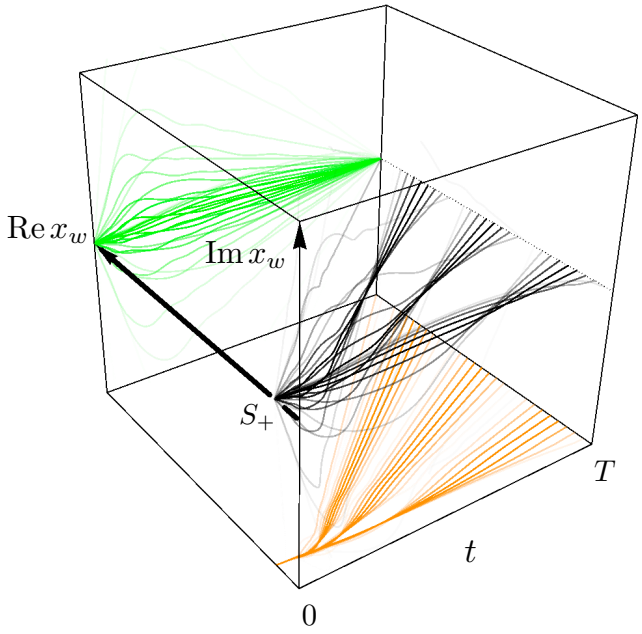

Figure 4.8: The weak value for position $x_w(t)$ in the complex plane for a number of different post-selections with the density proportional to the transition probability $|\langle x_f|U(T)|x_i\rangle|^2$. The real and imaginary parts are described in orange and green lines and projected on the bottom and the left-back planes, respectively.

In chapter 3, we have treated the interference. Let us briefly mention the interference. In classical optics, the interference results in the interference between the light reflected on the wall and straightly toward the screen. However, in this case, a infinite number of the paths are interfered each other, and the interference pattern is appeared on the screen.

4.9 Summary

In this chapter, we have shown the behavior of the weak value $x_w(t)$ in several models including multiple-slit (thought) experiment and Lloyd's mirror experiment. In the double-slit experiment, we have found that the real and imaginary parts of the weak values can be regarded as the average of the classical trajectory and the interference effect, respectively. The real part of the position weak value Re $x_w(t)$, however, cannot be interpreted as the average of the classical trajectory if we consider multiple (more than two) slit experiment. We found that the averaged nature of the weak value is rediscovered when one admits the complex probability. Then, quantum eraser is utilized to obtain which-path information. At the slit one can distinguish the particle, but, which path the particle takes is completely erased by the post-selection at the screen, and the interference fringes can be observed [7]. Although the which-path information seems to be completely lost in quantum eraser, by employing the spin-tagged position weak value, we can find which path the particle takes for an ensemble

without destroying interference. Since the weak value is defined for an ensemble not for individual event, this result does not contradict the complementarity. Finally, we have examined the weak value $x_w(t)$ with a non-vanishing potential, $V(x) = \infty$ for $x \leq 0$, which is known as Lloyd's mirror. The weak value $x_w(t)$ is a smooth function of time t and has a complex number in general even though $x_w(t)$ is real at each boundary.

Chapter 5

Conclusion and discussions

The aim of the present thesis is to interpret several quantum phenomena based on the weak values and thereby clarify the role of the weak value in quantum mechanics. It is pointed out that the weak value is useful to understand quantum mechanics intuitively. In particular, we have focused on the time-dependent position weak value and regarded it as the weak trajectory because in several examples the weak trajectory coincides with the classical trajectory. We all know that defining the trajectory is impossible in quantum mechanics because of the uncertainty principle. Similarly, we are aware of the difficulty of determining path of the particle in the double-slit experiment. The weak value, however, is defined in the weak limit not disturbing the initial state, so that we can obtain the values of noncommuting observables. Namely, without destroying the interference we can observe the position weak value. We have investigated the interference effect of the particle, because quantum interference is a quintessential phenomenon in quantum mechanics as Feynman pointed out [2].

To discuss interference, the path between the pre- and post-selections is defined by decomposing the transition probability in terms of a certain basis. Then, we have shown that the imaginary part of the weak value is related to the index of interference [29]. As examples, the double-slit (thought) experiment and the spin-1/2 system are examined. In the double-slit experiment, the index of interference is expressed in terms of the imaginary part of the momentum weak value alongside the screen. When the interference is destructive, the index of the interference (the imaginary part of the momentum weak value) diverges. Also, the imaginary part of the position weak value can be related to the index of interference through a dynamical relationship. In contrast, the index of the interference becomes zero when the interference becomes constructive. In addition, the spin-1/2 state has been investigated. The post-selected state is slightly rotated around a certain basis. The index of the interference is described by the imaginary part of the spin component.

To investigate the meaning of the real part, the position weak value is exploited, which we regard as the weak trajectory. We have shown that the weak trajectory between position eigenstates under the free Hamiltonian is purely real and coincides with the classical path. It seems that the weak value allows us to discuss the quantum path in the language of the classical world. To confirm this, we have studied multiple-slit (thought) experiment. In the double-slit experiment, the position weak value is just the average of the classical trajectories.

One may wonder if, in general, the real part of the position weak value is the average of the classical trajectories. This feature, however, does not hold for the three (or more) slit experiment. Nonetheless, the position weak value can be seen as the average of the classical trajectory if one admits the complex probability. We also have shown that the imaginary part of the weak value $x_w(t)$ can be related to the indicator of interference effect, i.e., the imaginary part vanishes when the interference becomes extremal [30]. So far, our argument is restricted to the multiple-slit experiment, but by extending the pre-selected state to the arbitrary one, this interpretation of the imaginary part of the weak value $x_w(t)$ can also be established. Indeed, for the momentum eigenstate and the complex Gaussian state, we have confirmed that the conclusion obtained above is valid.

At this point, the position weak value can be interpreted as the average, but we cannot specify which path the particle has taken. We have introduced the particle with a spin degrees of freedom so that we can obtain the which-path information we want. If one measures the spin state other than its position on the screen, the interference pattern will be washed away. Interference also cannot be observed when one obtains the which-path information. To preserve the interference pattern, we may choose to erase the which-path information. When this is done, we are usually unable to predict the trajectory of the particle for each event. In terms of the weak value, however, we can recover the capability of telling which path the particle takes without destroying the interference pattern. If the weak value is "re-scaled", the position weak value coincides with the classical trajectory. Obtaining its trajectory without destroying interference does not contradict the complementarity, because the weak value is defined for an ensemble, not for an individual event [29, 30].

Up to this point, our argument is restricted to the free Hamiltonian. We have shown another example, Lloyd's mirror, that causes an interference pattern on the screen. In classical optics, the paths can be described either by one which straightforwardly moves toward the screen or the other which is reflected by a wall (this is not a smooth function). In quantum mechanics, Lloyd's mirror can be expressed by a perfectly reflecting wall potential, and the Feynman kernel (propagator) for this potential has been already known. The position weak value can be numerically calculated, and it has turned out that the weak value has an imaginary part and is a smooth function of time. The behavior of the imaginary part of the weak value $x_w(t)$ is not trivial, but we can predict whether $x_w(t)$ has an imaginary or not by simply taking the derivative of the transition probability with respect to x_f (final position of the particle), and we find that $x_w(t)$ has the imaginary part generally. Consequently, the connection between the imaginary part and the interference is confirmed [30]. Although our analysis is based on some assumptions, the results we obtained allow us to understand the motion of the quantum particle more intuitively. It is obvious that, in order to understand the weak value or quantum trajectories more deeply, far more general cases should be examined.

Since the weak value is obtained under the weak limit, we may say that the weak measurement allows us to peep at the intermediate value which cannot be achieved by the strong measurement. Ideally, the weak value does not depend on the type of weak measurement one performs, which implies that the weak value represents some sort of physical value for the ensemble.

Our purpose of the present paper has been to make clear the role of the weak value in

quantum mechanics and thereby to comprehend the quantum phenomena intuitively. We have successfully explained the interpretation of the imaginary part which has been regarded to be obscure up to this point. Besides, we have shown that the weak value can be understood by the average of the classical value in several special cases. Our study suggests that the weak value can be regarded as a reasonable physical quantity. To elaborate our discussion, more general potential should be studied. It is our hope that our study can provide a help to assign a role of weak values in quantum mechanics.

Acknowledgement

First and foremost, I would like to express my special appreciation and thanks to my supervisor Professor Dr. I. Tsutsui. Without his supervision and constant help this dissertation would not have been possible. I would like to thank him for encouraging my research.

I am also grateful to T. Morita, K. Fukuda, J. Lee, R. Koganezawa, K. Matsuhisa, and N. Morisawa, for their support, feedback, and friendship. In addition, I would like to thank my fellows M. Yata, A. Konishi, T. Arai, Y. Sakaki, S. Ozaki, T. Takabe for helping me get through the difficult times, and for all the emotional support, and entertainment they provided.

Finally, I owe much to my parents, without their support and understanding I would not have completed this work.

Appendix A

Weak measurement (detailed calculation)

In section 2.5, we omitted the detailed calculation of the joint probability. In this appendix We will show the detailed derivation.

The joint probability is expressed as

$$\begin{aligned} P(\sigma_x, f) &= \mathrm{Tr}_s\left[\mathrm{Tr}_d\left[(|\sigma_x\rangle\langle\sigma_x| \otimes \Pi_f) U_w \rho(t) U_w^\dagger\right]\right] \\ &= \mathrm{Tr}_s\left[\mathrm{Tr}_d\left[U_w^\dagger (|\sigma_x\rangle\langle\sigma_x| \otimes \Pi_f) U_w \rho(t)\right]\right], \end{aligned} \tag{A.1}$$

where

$$\begin{aligned} &U_w^\dagger (|\sigma_x = +1\rangle\langle\sigma_x = +1| \otimes \Pi_f) U_w \\ &= \frac{1}{2} \begin{pmatrix} \cos(gA)\Pi_f \cos(gA) - \sin(gA)\Pi_f \cos(gA) & \cos(gA)\Pi_f \cos(gA) - \sin(gA)\Pi_f \cos(gA) \\ -\cos(gA)\Pi_f \sin(gA) + \sin(gA)\Pi_f \sin(gA) & +\cos(gA)\Pi_f \sin(gA) - \sin(gA)\Pi_f \sin(gA) \\ \\ \cos(gA)\Pi_f \cos(gA) - \sin(gA)\Pi_f \cos(gA) & \cos(gA)\Pi_f \cos(gA) + \sin(gA)\Pi_f \cos(gA) \\ +\cos(gA)\Pi_f \sin(gA) - \sin(gA)\Pi_f \sin(gA) & +\cos(gA)\Pi_f \sin(gA) + \sin(gA)\Pi_f \sin(gA) \end{pmatrix}. \end{aligned}$$

By using following relations

$$\begin{aligned} \cos(gA) &= \sum_{n=0}^{\infty} \frac{(gA)^{2n}}{(2n)!} = 1 + \sum_{n=1}^{\infty} \frac{g^{2n}}{(2n)!} A & \text{(A.2)} \\ &= 1 - A + A\cos g, & \text{(A.3)} \\ \sin(gA) &= A \sin g, & \text{(A.4)} \end{aligned}$$

the joint probability is

$$
\begin{aligned}
P(\sigma_x = +1, f) &= \mathrm{Tr}\left[\frac{1}{2}|\phi(t)\rangle\langle\phi(t)|\Big(\cos(gA)\Pi_f\cos(gA) + \sin(gA)\Pi_f\cos(gA)\right. \\
&\qquad \left. + \cos(gA)\Pi_f\sin(gA) + \sin(gA)\Pi_f\sin(gA)\Big)\right] \\
&= \mathrm{Re}[\sin g\langle\phi(t)|A|\psi(T-t)\rangle(\langle\psi(T-t)|\phi(t)\rangle + (-1+\cos g)\langle\psi(T-t)|A|\phi(t)\rangle)] \\
&\quad +\frac{1}{2}\sin^2 g|\langle\psi(T-t)|A|\phi(t)\rangle|^2 \\
&\quad +\frac{1}{2}|\langle\psi(T-t)|\phi(t)\rangle + (-1+\cos g)\langle\psi(T-t)|A|\phi(t)\rangle|^2 \qquad \text{(A.5)} \\
&= \frac{1}{2}|\langle\psi(t-t)|\phi(t)\rangle + (\sin g + \cos g - 1)\langle\psi(T-t)|A|\phi(t)\rangle|^2. \qquad \text{(A.6)}
\end{aligned}
$$

Similarly, other joint probabilities can be obtained.

Appendix B

Interference of quantum eraser

In this appendix, we show the relation between the quantum interference and the imaginary part of the weak value for the double-slit experiment in which we can observe the spin-tagged position weak value.

The pre-selected state at $t = 0$ is expressed by the superposition of two position eigenstates with the spin states $|\pm\rangle$,

$$|\phi\rangle = \frac{1}{\sqrt{2}}(|x_i\rangle \otimes |+\rangle + |-x_i\rangle \otimes |-\rangle), \tag{B.1}$$

while the post-selection is

$$|\psi\rangle = \frac{1}{\sqrt{2}}|x_f\rangle \otimes (|+\rangle + |-\rangle), \tag{B.2}$$

so that the interference pattern can be observed. When the state evolves under the free Hamiltonian, the transition probability is

$$|\langle\psi|U(T)|\phi\rangle|^2 = \frac{m}{2\pi\hbar T}\cos^2\left(\frac{m}{\hbar}\frac{x_f x_i}{T}\right). \tag{B.3}$$

Let us define the spin-tagged momentum operators,

$$p^{\pm} = p \otimes |\pm\rangle\langle\pm|. \tag{B.4}$$

The momentum operator p is sum of $p^{\pm}$,

$$p \otimes \mathbb{I} = p^{+} + p^{-}. \tag{B.5}$$

We begin by defining the translation operator $u_{p^{\pm}}(\alpha)$

$$u_{p^{\pm}}(\alpha) := \exp\left[-i\alpha p^{\pm}\right], \tag{B.6}$$

which translates the position of the particle with the spin $|\pm\rangle$ by α, then the transition amplitude between the pre- and post-selected states can be expressed,

$$K_{\pm}(\alpha) := \langle\psi|u_{p^{\pm}}(\alpha)U(T)|\phi\rangle. \tag{B.7}$$

To observe interference, we introduce an identity operator to divide the transition amplitude $K_{\pm}(\alpha)$,

$$\mathbb{I} = \int_0^\infty dx|x\rangle\langle x| + \int_{-\infty}^0 dx|x\rangle\langle x|. \tag{B.8}$$

Let us substitute the identity operator (B.8) to (B.7). Then the transition amplitude is split into to two parts,

$$\begin{aligned} K_{\pm}(\alpha) &= \langle\psi|u_{p^{\pm}}(\alpha)U(T)|\phi\rangle \\ &= \frac{\langle\psi|u_{p^{\pm}}(\alpha)U(T)|-x_i\rangle\otimes|+\rangle}{\sqrt{2}} + \frac{\langle\psi|u_{p^{\pm}}(\alpha)U(T)|x_i\rangle\otimes|-\rangle}{\sqrt{2}}. \end{aligned} \tag{B.9}$$

By using new states $|\phi_{\pm}\rangle = |\pm x_i\rangle\otimes|\pm\rangle/\sqrt{2}$, we define transition amplitudes,

$$K_{\pm,\mp}(\alpha) := \langle\psi|u_{p^{\pm}}(\alpha)U(T)|\phi_{\mp}\rangle. \tag{B.10}$$

The interference is caused by the phase difference between $K_{\pm,+}(\alpha)$ and $K_{\pm,-}(\alpha)$. In the case of this example, the post-selected state is eigenstate of the position $|x_f\rangle$. The weak value of momentum p_w, p_w^+ and p_w^- are

$$p_w^+ = \frac{\langle\psi|p^+U(T)|\phi\rangle}{\langle\psi|U(T)|\phi\rangle} = m\frac{x_f - x_i}{T(1+\mathrm{e}^{\mathrm{i}\chi})}, \tag{B.11}$$

$$p_{\pm_w} = \frac{\langle\psi|pU(T)|\phi_{\pm}\rangle}{\langle\psi|U(T)|\phi_{\pm}\rangle} = m\frac{x_f \mp x_i}{T}, \tag{B.12}$$

where χ is equal to the $2mx_fx_i/\hbar T$. Since the imaginary part of the spin-tagged momentum weak values $p_w^{\pm}$ are zero, the index of interference (3.11) for the translation of the particle with the spin $|+\rangle$ becomes

$$\begin{aligned} \mathcal{I} &= \mathrm{Im}\left[p_w^+ - p_{-_w}\frac{|K_{+,-}(0)|^2}{|K(0)|^2} - p_{+_w}\frac{|K_{+,+}(0)|^2}{|K(0)|^2}\right] \\ &= \mathrm{Im}\left[p_w^+\right] = \frac{m}{2}\frac{(x_f - x_i)\tan\left(\frac{m}{\hbar}\frac{x_fx_i}{T}\right)}{T}, \end{aligned} \tag{B.13}$$

from which the variation of interference terms is represented by the imaginary part of the weak value p_w^+. The variation of interference fringes correspond to the imaginary part of the weak value p_w^+.

Since we have (4.8), we can safely say that the derivative of the spin-tagged position weak value $x_w^+(t)$ with respect to time t is proportional to the spin-tagged momentum weak value p_w^+. Thus, the imaginary part of the spin-tagged position weak value $\mathrm{Im}\, x_w^+(t)$ can be regarded as the interference effect.

Reference

[1] L. De Broglie, Found. Phys. **1**, 5 (1970).

[2] L. Feynman and R. Leighton, *Sands, The Feynman Lectures on Physics Vol. 3*, Addison-Wesley, 1964.

[3] C. Jonsson, Zeitschrift für Physik **161**, 454 (1961).

[4] A. Tonomura, J. Endo, T. Matsuda, T. Kawasaki, and H. Ezawa, Am. J. Phys. **57**, 117 (1989).

[5] Y. Aharonov and D. Bohm, Phys. Rev. **115**, 485 (1959).

[6] A. Tonomura et al., Phys. Rev. Lett. **56**, 792 (1986).

[7] M. O. Scully, B.-G. Englert, and H. Walther, Nature **351**, 111 (1991).

[8] S. Kocsis et al., Science **332**, 1170 (2011).

[9] H. M. Wiseman, New J. Phys. **9**, 165 (2007).

[10] D. Bohm, Phys. Rev. **85**, 166 (1952).

[11] D. Bohm, Phys. Rev. **85**, 180 (1952).

[12] C. Philippidis, C. Dewdney, and B. J. Hiley, Il Nuovo Cimento B Series 11 **52**, 15 (1979).

[13] Y. Aharonov, D. Z. Albert, and L. Vaidman, Phys. Rev. Lett. **60**, 1351 (1988).

[14] O. Hosten and P. Kwiat, Science **319**, 787 (2008).

[15] P. B. Dixon, D. J. Starling, A. N. Jordan, and J. C. Howell, Phys. Rev. Lett. **102**, 173601 (2009).

[16] J. S. Lundeen, B. Sutherland, A. Patel, C. Stewart, and C. Bamber, Nature **474**, 188 (2011).

[17] L. Hardy, Phys. Rev. Lett. **68**, 2981 (1992).

[18] K. Mølmer, Phys. Lett. A **292**, 151 (2001).

[19] Y. Aharonov, A. Botero, S. Popescu, B. Reznik, and J. Tollaksen, Phys. Lett. A **301**, 130 (2002).

[20] J. Lundeen and A. Steinberg, Phys. Rev. Lett. **102**, 020404 (2009).

[21] A. Danan, D. Farfurnik, S. Bar-Ad, and L. Vaidman, Phys. Rev. Lett. **111**, 240402 (2013).

[22] Y. Aharonov, P. Bergmann, and J. Lebowitz, Phys. Rev. **134**, B1410 (1964).

[23] Y. Aharonov and L. Vaidman, Phys. Rev. A **41**, 11 (1990).

[24] Y. Aharonov, S. Popescu, D. Rohrlich, and P. Skrzypczyk, New J. Phys. **15**, 113015 (2013).

[25] T. Denkmayr et al., Nat. Commun. **5** (2014).

[26] Y. Aharonov and A. Botero, Phys. Rev. A **72**, 052111 (2005).

[27] J. Dressel and A. Jordan, Phys. Rev. A **85**, 012107 (2012).

[28] L. Vaidman, Found. Phys. **26**, 895 (1996).

[29] T. Mori and I. Tsutsui, arXiv preprint arXiv:1410.0787 (2014).

[30] T. Mori and I. Tsutsui, arXiv preprint arXiv:1412.0916 (2014).

[31] B. Reznik and Y. Aharonov, Phys. Rev. A **52**, 2538 (1995).

[32] A. Einstein, B. Podolsky, and N. Rosen, Phys. Rev. **47**, 777 (1935).

[33] J. S. Bell et al., Physics **1**, 195 (1964).

[34] M. Redhead, *Incompleteness, nonlocality, and realism: a prolegomenon to the philosophy of quantum mechanics*, Clarendon Press, 1987.

[35] S. Wu and K. Mølmer, Phys. Lett. A **374**, 34 (2009).

[36] H. F. Hofmann, New J. Phys. **13**, 103009 (2011).

[37] A. Tanaka, Phys. Lett. A **297**, 307 (2002).

[38] T. Morita, T. Sasaki, and I. Tsutsui, Progr. Theor. Exp. Phys. **2013**, 053A02 (2013).

[39] M. O. Scully and K. Drühl, Phys. Rev. A **25**, 2208 (1982).

[40] P. G. Kwiat, A. M. Steinberg, and R. Y. Chiao, Phys. Rev. A **45**, 7729 (1992).

[41] T. J. Herzog, P. G. Kwiat, H. Weinfurter, and A. Zeilinger, Phys. Rev. Lett. **75**, 3034 (1995).

[42] T. Fülöp and I. Tsutsui, Phys. Lett. A **264**, 366 (2000).